



MICROFLOW ELECTROCHEMICAL DETECTION ON CLOTH-BASED  
DEVICE

TANAPORN BOONNIKOM

A THESIS SUBMITTED IN PARTIAL FULFILLMENT OF  
THE REQUIREMENTS FOR MASTER DEGREE OF SCIENCE  
IN CHEMISTRY

FACULTY OF SCIENCE  
BURAPHA UNIVERSITY

2024

COPYRIGHT OF BURAPHA UNIVERSITY



ไมโครโพลที่มีการตรวจวัดแบบเคมีไฟฟ้าบนอุปกรณ์แบบผ้า



ธนพร บุญนิคม

วิทยานิพนธ์นี้เป็นส่วนหนึ่งของการศึกษาตามหลักสูตรวิทยาศาสตรมหาบัณฑิต

สาขาวิชาเคมี

คณะวิทยาศาสตร์ มหาวิทยาลัยบูรพา

2567

ลิขสิทธิ์เป็นของมหาวิทยาลัยบูรพา

MICROFLOW ELECTROCHEMICAL DETECTION ON CLOTH-BASED  
DEVICE



TANAPORN BOONNIKOM

A THESIS SUBMITTED IN PARTIAL FULFILLMENT OF  
THE REQUIREMENTS FOR MASTER DEGREE OF SCIENCE  
IN CHEMISTRY  
FACULTY OF SCIENCE  
BURAPHA UNIVERSITY

2024

COPYRIGHT OF BURAPHA UNIVERSITY

The Thesis of Tanaporn Boonnikom has been approved by the examining committee to be partial fulfillment of the requirements for the Master Degree of Science in Chemistry of Burapha University

Advisory Committee

Examining Committee

Principal advisor

.....  
(Associate Professor Dr. Yupaporn Sameenoi)

..... Principal examiner  
(Assistant Professor Dr. Nathawut Choengchan)

..... Member  
(Assistant Professor Dr. Napa Tangtreamjitmun)

..... Member  
(Associate Professor Dr. Yupaporn Sameenoi)

..... Dean of the Faculty of Science  
(Associate Professor Dr. Usavadee Tuntiwaranuruk)

This Thesis has been approved by Graduate School Burapha University to be partial fulfillment of the requirements for the Master Degree of Science in Chemistry of Burapha University

..... Dean of Graduate School  
(Associate Professor Dr. Witawat Jangiam)

65910109: MAJOR: CHEMISTRY; M.Sc. (CHEMISTRY)

KEYWORDS: CLOTH-BASED DEVICE; MICROFLOW INJECTION ANALYSIS; ELECTROCHEMICAL DETECTION

TANAPORN BOONNIKOM : MICROFLOW ELECTROCHEMICAL DETECTION ON CLOTH-BASED DEVICE. ADVISORY COMMITTEE: YUPAPORN SAMEENOI, Ph.D. 2024.

A continuous flow-electrochemical microfluidic cloth-based device (CF- $\mu$ CAD) has been developed to create microflow injection analysis ( $\mu$ FIA) system with integrated electrochemical detection on the cloth-based device (CAD). The  $\mu$ CAD was designed to have a long channel to allow the capillary flow and fabricated by polymer screen-printing method using polystyrene as a hydrophobic material. The electrode was screen-printed on the CAD at the end of the channel using silver-silver chloride, carbon paste modified with Prussian blue, and carbon paste as reference, working, and auxiliary electrodes, respectively. A  $\mu$ FIA system is created by immersing the top end in a microtube containing the carrier solution. The area next to the electrode is inclined at an angle of 45 degrees to the plane and the end of the channel is dipped in the lower reservoir. The flow analysis was performed by injecting the analyte at the sample injection zone which is located 1.0 cm away from the reference electrode. The solution flowed on the CAD by the capillary wicking, and the gravitational force from the carrier's upper reservoir and pushed the analyte to pass through the electrodes to the lower reservoir. Under optimal conditions, the system was applied for analysis of  $H_2O_2$ , glucose and pesticide in food, human serum and rice field water sample, respectively. The method provided accurate analysis of these analyte comparable to the traditional methods or certified values. These results indicated that the developed CF- $\mu$ CAD can served as an analytical platform that can be applicable in a wide range of chemical analysis and can be extensively used in the future.

## ACKNOWLEDGEMENTS

First of all, I extend my heartfelt gratitude and sincere appreciation to my advisor, Assoc. Prof. Dr. Yupaporn Sameenoi for her invaluable guidance, unwavering support, encouragement, and insightful advice throughout my study and research journey. Great appreciation is offered to all committee members for thesis defense, Asst. Prof. Dr. Nathawut Choengchan and Asst. Prof. Dr. Napa Tangtreamjitmun for their valuable feedback, and constructive criticism. Their expertise and insights have greatly contributed to the development and refinement of my work. And a special thank you to Miss Benjarat Tasangtong for her invaluable advice, guidance, support, and encouragement throughout the research.

I would like to acknowledge (i) Scholarship Support from Burapha University (ii) the Center of Excellence for Innovation in Chemistry (PERCH-CIC), Commission on Higher Education, Ministry of Education, Thailand (iii) Science Innovation Facility, Faculty of Science, Burapha University for the supports throughout my research. I also would like to thank the Department of Chemistry, Faculty of Science, Burapha University, Thailand where I obtained very good experiences.

Finally, I would like to express my deepest gratitude to my beloved family for their unwavering encouragement, boundless support, and invaluable assistance throughout my journey to obtain my master's degree. Their constant encouragement and unwavering belief in my abilities have been a driving force behind my success. Their love, support, and sacrifices have been instrumental in helping me navigate the challenges and achieve my goals. I am profoundly grateful for their endless encouragement and motivation, without which this success would not have been possible.

Tanaporn Boonnikom

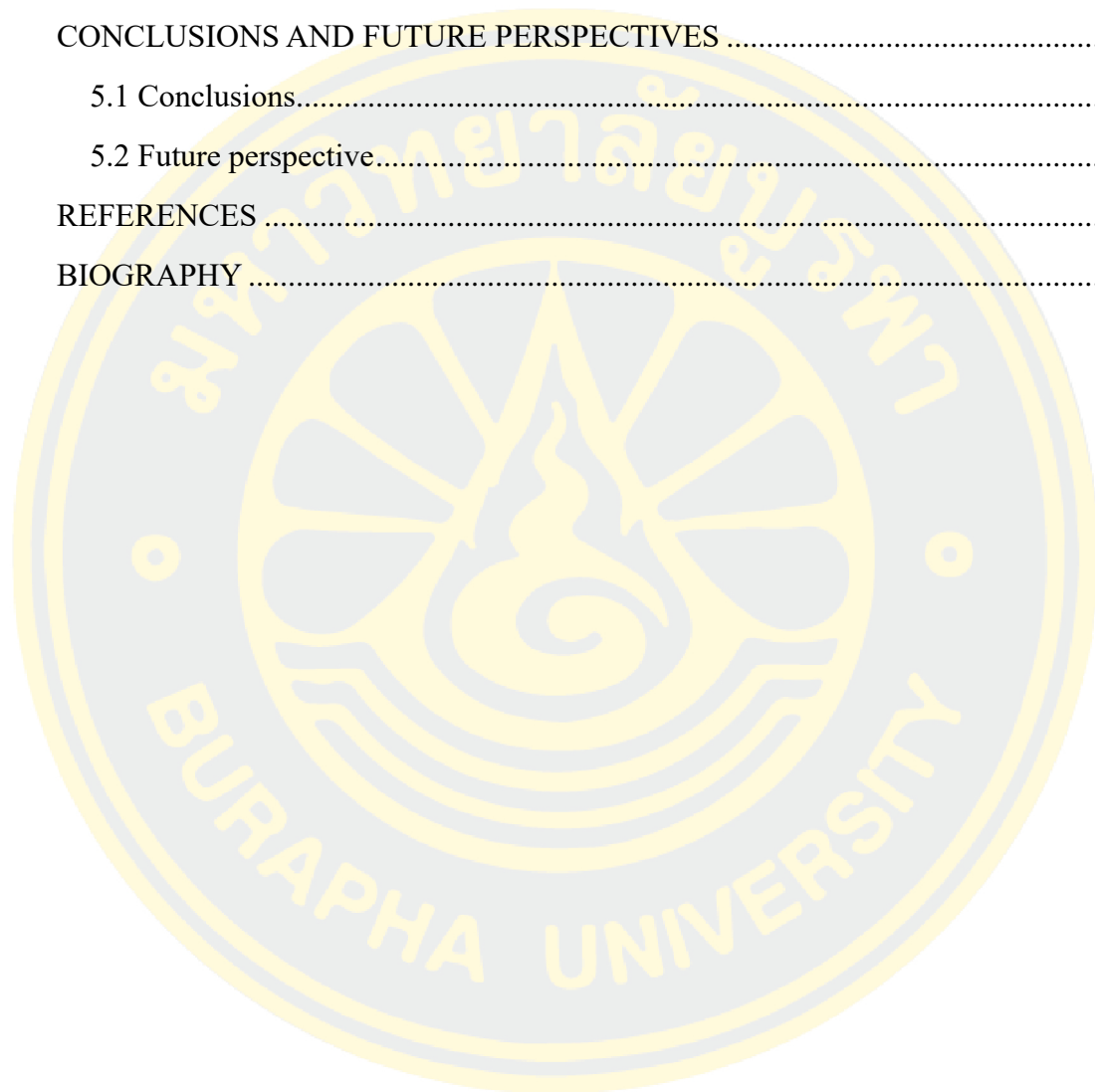
## TABLE OF CONTENTS

	<b>Page</b>
ABSTRACT.....	D
ACKNOWLEDGEMENTS.....	E
TABLE OF CONTENTS.....	F
LIST OF TABLES.....	J
LIST OF FIGURES.....	K
CHAPTER 1.....	1
INTRODUCTION.....	1
1.1 Research Background.....	1
1.2 Objective.....	2
1.3 Scope to study.....	3
1.4 Contribution to knowledge.....	3
CHAPTER 2.....	4
LITERATURE REVIEW.....	4
2.1 Flow injection analysis; FIA.....	4
2.2 Microflow injection analysis; $\mu$ FIA.....	5
2.3 Cloth-based analytical device; $\mu$ CAD.....	6
2.4 Microfluidic Systems with Amperometric Detection.....	8
2.5 Related literature reviews.....	10
CHAPTER 3.....	21
EXPERIMENTAL.....	21
3.1 Materials and chemicals.....	21
3.1.1 Materials.....	21
3.1.2 Chemicals.....	21
3.1.3 Real samples.....	22
3.2 Research plan.....	23

3.3 Preparation of solutions .....	24
3.3.1 Polystyrene solution 35% (w/v) .....	24
3.3.2 Sodium carbonate ( $\text{Na}_2\text{CO}_3$ ) solution.....	24
3.3.3 Electrodes containing carbon paste 0.8 g and Prussian blue 0.2 g .....	24
3.3.4 Potassium nitrate solution .....	24
3.3.5 Hydrogen peroxide solution .....	24
3.3.6 Hydrochloric acid solution .....	24
3.3.7 Tris buffer solution pH 7.4 .....	24
3.3.8 Bovine serum albumin; BSA in Tris buffer solution .....	25
3.3.9 Acetylthiocholine solution.....	25
3.3.10 Acetylcholinesterase Enzyme (AChE) .....	25
3.3.11 Pesticide standard Chlorpyrifos-oxon (CPO).....	25
3.3.12 Dithiothreitol solution (DTT).....	25
3.3.13 Glucose solution .....	25
3.3.14 Bovine serum albumin; BSA in 0.1 M phosphate buffer solution pH 7.25	
3.3.15 Glucose Oxidase (Gox) .....	26
3.4 Design and fabrication of cloth-based devices. ....	26
3.5 Fabrication of electrodes using stencil transparent film-printing method on cloth ( $\mu\text{CAD}$ ) .....	27
3.6 Electrochemical characterization on cloth-based devices by cyclic voltammetry .....	28
3.7 Microflow injection analysis on cloth devices .....	28
3.7.1 Optimum conditions analysis with microflow injection analysis.....	30
3.7.1.1 Optimum injection volume of sample solution .....	30
3.7.1.2 Optimum injection distance of sample solution .....	30
3.7.1.3 Optimum Incline angle electrode area of the cloth-based device.	30
3.8 Application of the developed microflow system .....	30
3.8.1 Hydrogen peroxide detection .....	30
3.8.1.1 Applied potential .....	30
3.8.1.2 Analysis of $\text{H}_2\text{O}_2$ using the CF- $\mu\text{CAD}$ system .....	31

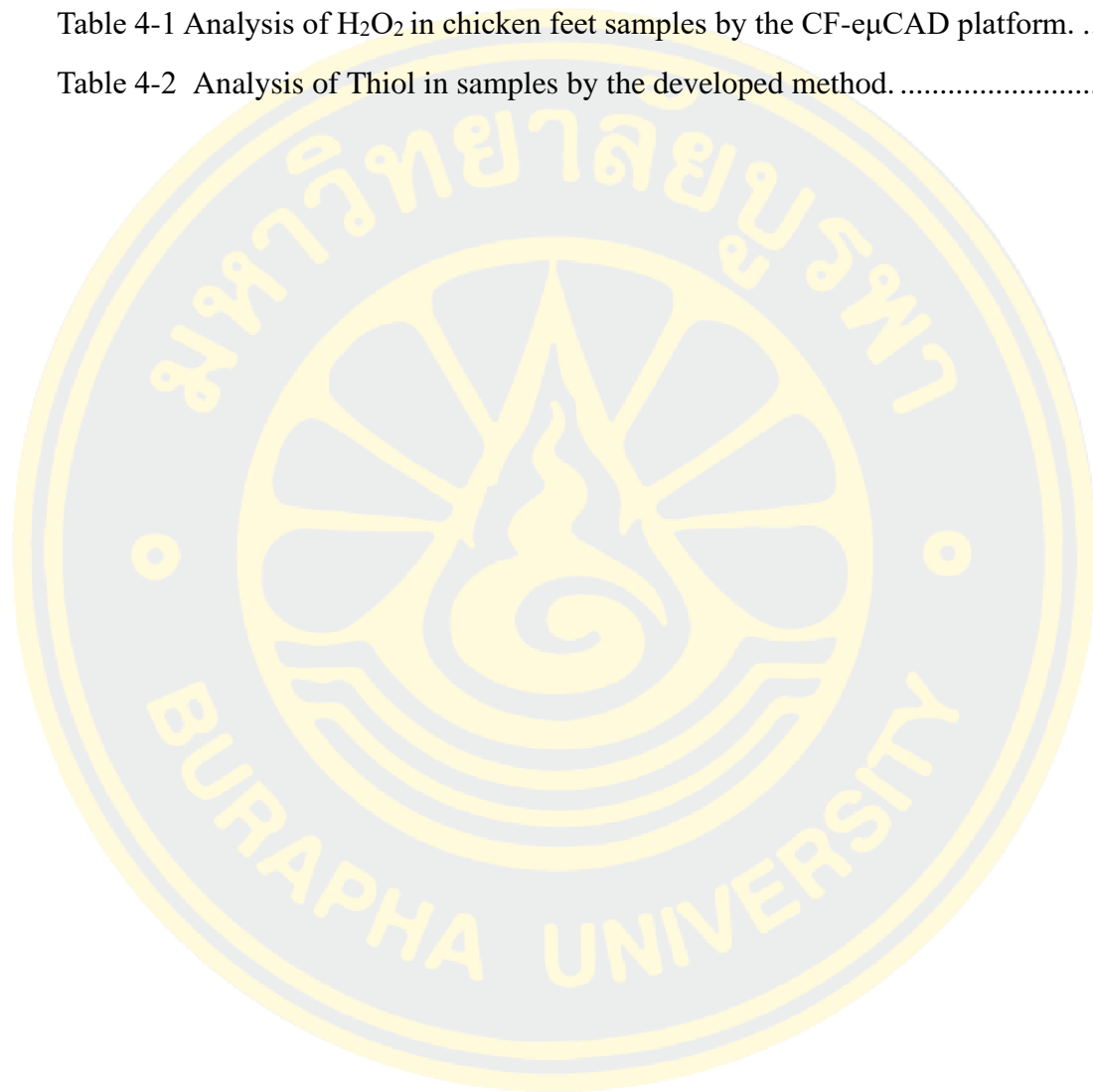
3.8.2 Glucose detection .....	31
3.8.3 Organophosphate pesticide detection .....	31
3.8.3.1 Applied potential .....	31
3.8.3.2 Analysis of organophosphate pesticide using the CF-e $\mu$ CAD system .....	32
3.8.3 Analytical features for the analysis of H <sub>2</sub> O <sub>2</sub> , glucose and organophosphate pesticide using the CF-e $\mu$ CAD system.....	33
3.8.3.1 Repeatability .....	33
3.8.3.2 Limit of Detection and Quantification: LOD, LOQ .....	33
CHAPTER 4 .....	34
RESULTS AND DISCUSSION.....	34
4.1 Electrochemical characterization on cloth-based sensor by cyclic voltammetry .....	34
4.2 Microflow injection analysis system optimization .....	35
4.2.1 Optimum injection volume of sample solution .....	35
4.2.2 Optimum injection distance of sample solution .....	36
4.2.3 Optimum Incline angle electrode area of the cloth-based device .....	37
4.3 Application of the developed microflow system .....	37
4.3.1 Hydrogen peroxide detection using the developed CF-e $\mu$ CAD system...38	
4.3.1.1 Applied potential .....	39
4.3.1.2 Linear range.....	39
4.3.1.3 Repeatability, Limit of Detection, and Limit of Quantification ...40	
4.3.2 Glucose detection using the developed CF-e $\mu$ CAD system.....41	
4.3.2.1 Linear range.....	42
4.3.2.2 Limit of Detection and Limit of Quantification .....	43
4.3.2.3 Glucose in human control serum analysis using the developed CF-e $\mu$ CAD system.....	43
4.3.3 Pesticide analysis using the developed CF-e $\mu$ CAD system.....43	
4.3.3.1 Applied potential .....	44
4.3.3.2 Linear range.....	44

4.3.3.3 Limit of Detection and Limit of Quantification .....	45
4.3.3.4 Analysis of organophosphate pesticide using the CF- $\mu$ CAD system .....	46
CHAPTER 5 .....	49
CONCLUSIONS AND FUTURE PERSPECTIVES .....	49
5.1 Conclusions.....	49
5.2 Future perspective.....	49
REFERENCES .....	50
BIOGRAPHY .....	54



## LIST OF TABLES

	<b>Page</b>
Table 4-1 Analysis of H <sub>2</sub> O <sub>2</sub> in chicken feet samples by the CF- $\mu$ CAD platform. ....	41
Table 4-2 Analysis of Thiol in samples by the developed method. ....	48



## LIST OF FIGURES

	<b>Page</b>
Figures 1-1 Design of the CF- $\mu$ CAD system.....	2
Figures 2-1 The components of the Flow Injection Analysis system. (Cerdà, Ferrer, Avivar, & Cerdà, 2014) .....	4
Figures 2-2 Cloth-based analytical device for colorimetric detection. (Nilghaz et al., 2012) .....	8
Figures 2-3 Microfluidic system of cotton thread Analyzed by amperometric technique. (Oliveira et al., 2019) .....	10
Figures 2-4 (I) The schematic diagram of CF-TPE-ePAD. (II) shows the image of the CF-TPE-ePAD characteristics. (Pradela-Filho et al., 2020).....	11
Figures 2-5 The influence of the paper substrate on the amperometric signal. (Pradela-Filho et al., 2020) .....	12
Figures 2-6 Schematic illustration of wax-screen-printing for fabrication of $\mu$ CADs. (1) The screen is placed over the cloth; (2) the screen is rubbed with a crayon and smooth utensil; (3) the cloth is placed on the heating board together with the screen; (4) the screen and cloth are removed from the heating board; (5) the patterned cloth is separated from the screen. (Guan et al., 2015) .....	13
Figures 2-7(A) The characteristics of a fabric-based device used for the analysis of $H_2O_2$ through chemiluminescence detection. The size of the detection area and the quantification of $H_2O_2$ on the fabric-based device are shown. (B) shows the detection and analysis of microfluidic chemiluminescence on the fabric-based device. (Guan et al., 2015) .....	14
Figures 2-8 Steps for assembling the wax-carbon electrode printed on paper and polymer substrate. (Godino et al., 2012) .....	15
Figures 2-9 Microfluidic system on a fabric-based device for electrochemical .....	16
Figures 2-10 A one-step screen printing method using polymer for the fabrication of microfluidic analysis devices with a microfiber cloth ( $\mu$ CADs). (Tasaengtong & Sameenoi, 2020a).....	17

Figures 2-11 Construction of $\mu$ TED with an inlet (a) and outlet reservoirs (b), injection zone (c), cavities for the accommodation of auxiliary and reference electrodes of cylindrical graphites (d), orifice for carbon paste accommodation (work electrode) (e) with a copper electrical contact (f) and textile threads (g). (Kalinke et al., 2019) .....	18
Figures 2-12 The Microfiber-based Electrochemical Detection Device ( $\mu$ TED) and its application in detection and measurement are reported in this article. (Kalinke et al., 2019) .....	19
Figures 2-13 Overview of FED technology. (a) The instrumental setup for lactate ...	20
Figures 3-1 Procedure for Fabrication of the $\mu$ CAD using the polymer screen printing method.....	26
Figures 3-2 Procedure for electrode fabrication using stencil lamination film printing. ....	27
Figures 3-3 Cyclic voltammetry measurement of the electrodes on the cloth-based devices.....	28
Figures 3-4 Microflow system for continuous-flow electrochemical cloth-based microfluidic analytical devices (CF- $\mu$ CADs). ....	29
Figures 3-5 Detection of organophosphate pesticides is conducted using the CF- $\mu$ CAD system through an enzymatic method. ....	32
Figures 4-1 (A) Representative cyclic voltammograms of the PB-modified carbon paste electrodes at different scan rates ((a) 5, (b) 10, (c) 25, and (d) 50 mV/s) in 1 M $\text{KNO}_3$ . (B) The relationship between anodic and cathodic currents and the square root of the scan rate. ....	35
Figures 4-2 The relationship between the reduction current (black) and peak width (orange) and the injection volume. (Applied potential: -0.30 V vs Ag/AgCl; $\text{H}_2\text{O}_2$ : 1.0 mM; Injection distance: 1 cm; Incline angle: 35 degree), (B) The signal of injection volume with amperometry. ....	36
Figures 4-3 (A) The relationship between of reduction current (black) and peak width (orange) as a function of sample injection distance (measured from reference electrode). (Applied potential: -0.30 V vs Ag/AgCl; $\text{H}_2\text{O}_2$ : 1.0 mM; Injection volume: 2.0 $\mu\text{L}$ ; Incline angle: 35 degree), (B) The signal of injection distance with amperometry. ....	36
Figures 4-4 (A) Relationship between the reduction current (black) and peak width (orange) and the inclined angle of the $\mu$ CAD. (Applied potential: -0.30 V vs Ag/AgCl;	

H <sub>2</sub> O <sub>2</sub> : 1.0 mM; Injection distance: 1.0 cm; Injection volume: 3.0 μL), (B) The signal of inclined angle of the μCAD with amperometry.....	37
Figures 4-5 Cyclic voltammogram obtained from analysis of H <sub>2</sub> O <sub>2</sub> (solid line) and KNO <sub>3</sub> (dash line) using the electrodes fabricated on cloth-based devices. Experimental conditions: Scanning potential: -1.2-1 V; Scan rate at 0.05 V/s; Step potential 0.002 V; Supporting electrolyte is KNO <sub>3</sub> concentration 1 M.....	38
Figures 4-6 Relationship between the signal to blank of H <sub>2</sub> O <sub>2</sub> and applied potential (V) (Supporting electrolyte: 1 M KNO <sub>3</sub> , Detection: 1 mM H <sub>2</sub> O <sub>2</sub> , injection volume: 3 μL, injection distance: 1 cm from RE). ....	39
Figures 4-7 (A) The signal of H <sub>2</sub> O <sub>2</sub> measured with amperometry. (B) Calibration curve of H <sub>2</sub> O <sub>2</sub> on a cloth-based device with microflow injection analysis. (Experimental conditions: Applied potential: -0.3 V vs. Ag/AgCl; Carrier solution: 1 M KNO <sub>3</sub> ; Injection volume: 3 μL; Injection distance: 1.0 cm; Inclined angle: 45 degree, n=3).....	40
Figures 4-8 (A) The signal of glucose solution measured with amperometry. (B) Calibration curve of glucose on a cloth-based device with microflow injection analysis. (Experimental conditions: Applied potential: -0.3 V vs. Ag/AgCl; Carrier solution: 1 M KNO <sub>3</sub> ; Injection volume: 3 μL; Injection distance: 1.0 cm; Inclined angle: 45 degree, n=3) .....	42
Figures 4-9 Relationship between the signal to blank of DTT and applied potential (V) (Supporting electrolyte: 1 M KNO <sub>3</sub> , Detection: 1 mM H <sub>2</sub> O <sub>2</sub> , injection volume: 3 μL, injection distance: 1 cm from RE). ....	44
Figures 4-10 (A) The signal of dithiothreitol solution measured with amperometry. (B) Calibration curve of dithiothreitol on a cloth-based device with microflow injection analysis. (Experimental conditions: Applied potential: +0.3 V vs. Ag/AgCl; Carrier solution: 1 M KNO <sub>3</sub> ; Injection volume: 3 μL; Injection distance: 1.0 cm; Inclined angle: 45 degree, n=3). ....	45
Figures 4-11 (A) The signal of chlorpyrifos-oxon (CPO) solution measured with amperometry. (B) Calibration curve of pesticide on a cloth-based device with microflow injection analysis. (Experimental conditions: Applied potential: -0.3 V vs. Ag/AgCl; Carrier solution: 1 M KNO <sub>3</sub> ; Injection volume: 3 μL; Injection distance: 1.0 cm; Inclined angle: 45 degree, n=3). ....	47

# CHAPTER 1

## INTRODUCTION

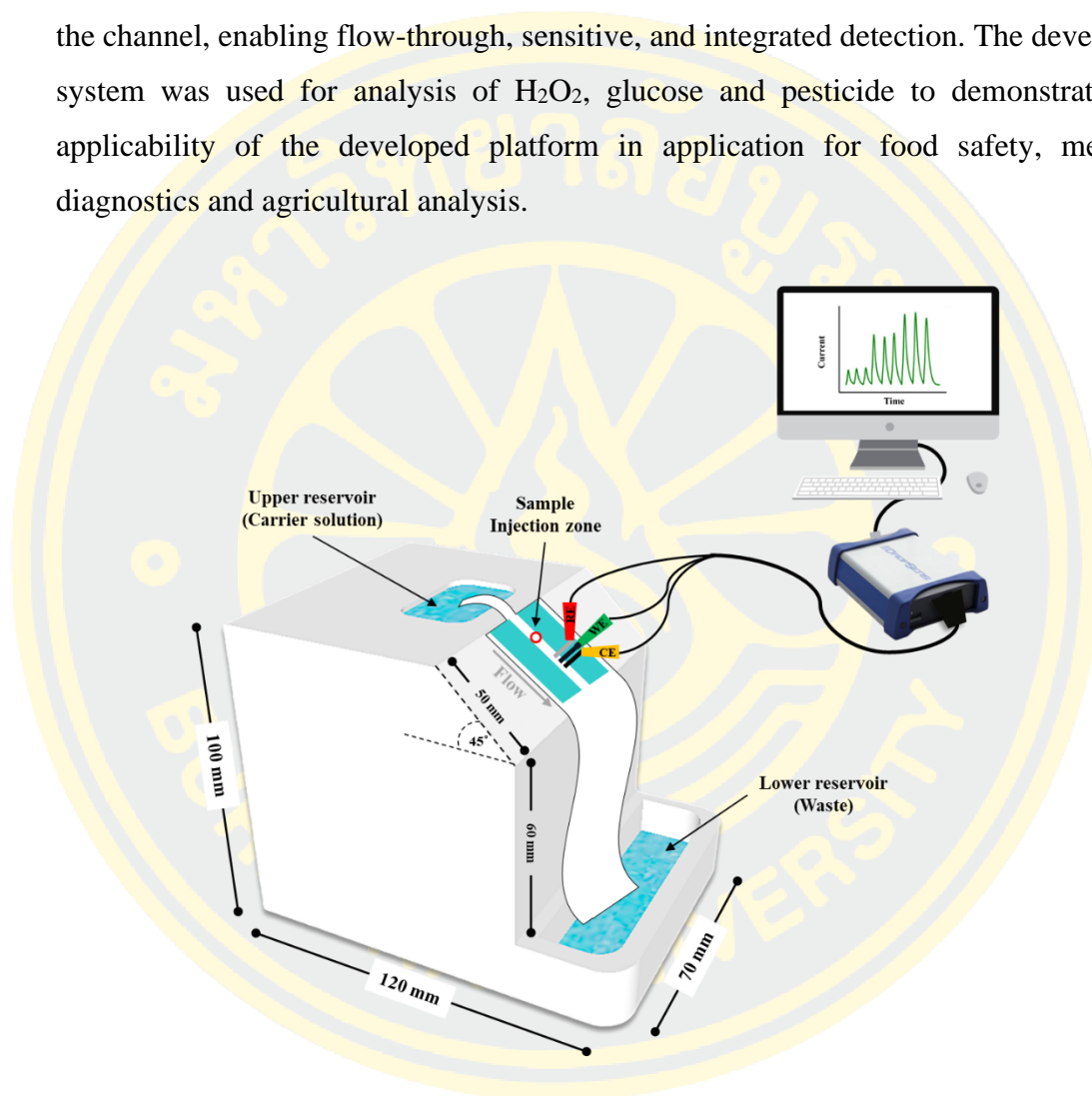
### 1.1 Research Background

Food and health are strongly tied to one another since consuming a nutritious diet of safe foods is essential to fostering good health. The World Health Organization (WHO) states that unsafe food can cause more than 200 different diseases, ranging from cancer to diarrhoea, by harboring dangerous bacteria, viruses, parasites, or chemicals. Around the world, fall ill after eating contaminated food each year, resulting deaths and the loss healthy. (WHO, 2020) Monitoring of food quality and safety are therefore necessary to prevent illness and mortality rate from consuming unsafe foods.

Traditional methods for food analysis, such as chromatography, spectrophotometry, electrophoresis, and titration, are typically performed in a laboratory setting and require well-trained personnel, resulting in long analysis times and high per-sample costs. As a result, they are not suitable for use in resource-poor areas. Microfluidic analysis systems offer a rapid, portable, and sensitive alternative to these traditional methods, making them ideal for use in remote regions and resource-limited countries. Recently, cloth has emerged as a viable material for creating microfluidic devices, known as microfluidic cloth-based analytical devices ( $\mu$ CADs), due to its low cost, widespread availability, and wicking properties that allow for capillary flow during analysis, eliminating the need for an external pump.

This project aims to use cloth as a microfluidic substrate to develop a novel, low-cost, and simple analytical platform called continuous flow electrochemical cloth-based microfluidic analytical devices (CF- $\mu$ CADs) for food analysis. While traditional flow injection analysis (FIA) platforms have been used for decades to automate routine analysis in laboratory settings for clinical diagnostics, environmental monitoring, and food analysis, their size and complexity limit their application for on-site monitoring. In contrast, the proposed CF- $\mu$ CADs system is a miniaturized microfluidic platform that improves portability, reduces sample consumption and analysis costs, and shortens analysis times.

Here, the cotton cloth was designed to have a narrow hydrophilic channel, allowing for the flow of the carrier from the upper to the lower reservoir by capillary wicking and gravitational force (Figure 1-1). Electrochemical detection was integrated on-chip, with electrode materials screen printed directly onto the  $\mu$ CAD at the end of the channel, enabling flow-through, sensitive, and integrated detection. The developed system was used for analysis of  $\text{H}_2\text{O}_2$ , glucose and pesticide to demonstrate the applicability of the developed platform in application for food safety, medical diagnostics and agricultural analysis.



Figures 1-1 Design of the CF- $\mu$ CAD system.

## 1.2 Objective

To create a cutting-edge analytical platform by designing and developing a novel microflow injection analysis system. This innovative platform used cloth as a substrate and was called the Continuous Flow Electrochemical Cloth-Based

Microfluidic Analytical Devices (CF- $\mu$ CADs). This novel approach allowed for rapid and sensitive analysis of food, biological and agricultural samples using electrochemical detection.

### **1.3 Scope to study**

1. Design and develop the CF- $\mu$ CADs using the screen-printing fabrication of  $\mu$ CAD and screen-printing electrode.
2. Study optimal condition for the developed analysis system including injection volume, injection distance, incline angle electrode and applied potential.
3. Apply the developed system for analysis of analyte standards including  $H_2O_2$ , glucose and pesticides.
4. Apply the developed system for analysis of  $H_2O_2$ , glucose and pesticides in real samples.

### **1.4 Contribution to knowledge**

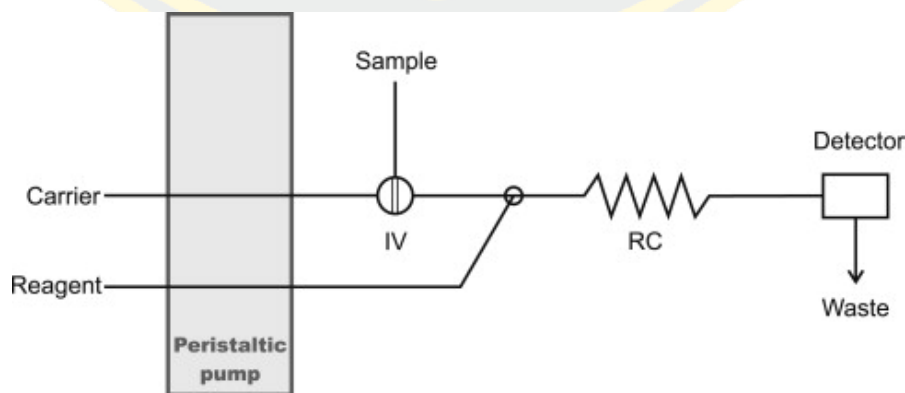
The microflow platform developed in this study is suitable for a rapid and sensitive analytical platform with low analysis costs and minimal consumption of samples and reagents. It can be further applied to a wide range of areas.

## CHAPTER 2

### LITERATURE REVIEW

#### 2.1 Flow injection analysis; FIA

The technique of Flow Injection Analysis (FIA) was first introduced in 1975 by Ruzicka and Hansen. The fundamental principle is based on the injection of a small amount of substance through an injection valve into the flow path of a chemical substance, which may be a reagent or a solvent that continuously flows at an appropriate and constant flow rate through a small-diameter tube (0.3-1.0 mm) without air bubbles. The flow of the carrier substance is controlled by using a peristaltic pump and the force of gravity. The sample substance is mixed with the carrier flow and undergoes a reaction at the mixing coil. The resulting product, such as light absorbance, electrical conductivity, and pH changes, then flows through the flow-through cell of the detector device, such as a UV-VIS spectrometer, conductivity meter, or pH meter, to measure the signal of the product. The appropriate detector must be selected to match the changes that occur. The resulting signal was in the form of a peak, which can be recorded and used to determine the quantity of the sample substance by comparing it to a standard graph. In addition, there must be control over various parameters that affect the analysis, such as the quantity of the sample substance, the concentration of the chemicals used, the size and length of the tubing used for the flow rate, the length of the mixing coil, and various interference factors.



Figures 2-1 The components of the Flow Injection Analysis system. (Cerdà, Ferrer, Avivar, & Cerdà, 2014)

## 2.2 Microflow injection analysis; $\mu$ FIA

Microflow injection analysis ( $\mu$ FIA) is an efficient technique that uses the same principles of traditional flow injection analysis (FIA) for flow analysis, but with all analysis components integrated into a microfluidic device. This device can perform continuous flow analysis similar to the FIA system, but with the advantage over the traditional FIA method of using smaller amounts of samples and reagents, at around 1000 times less. It enables fast analysis and is portable. The conventional microfluidic system was created using silicon, glass, and polymer and a photolithography technique to construct the device, which is an expensive and multi-step process that must be done in a standard clean room. When developing the  $\mu$ FIA system, external pumps are still required, and connecting the devices can be difficult due to the various tubes that need to be connected. Due to the small size of the equipment, it is necessary to find new methods or equipment that can analyze  $\mu$ FIA easily, with inexpensive materials and equipment. (Agustini, Bergamini, & Marcolino-Junior, 2016) (Zhang, Su, Liang, & Lai, 2020)

$\mu$ FIA involves the injection of a small volume of sample into a microchannel, followed by the addition of a reagent that reacts with the analyte of interest. The resulting reaction generates a signal that is detected using a suitable detector, such as a UV-Vis spectrophotometer or a fluorescence detector. (Peter R. Seidl, 1994) The microscale nature of  $\mu$ FIA allows for the use of small amounts of reagents and samples, reducing the amount of waste generated and lowering the cost of analysis. (Maria A. G. Soliva, 2017)

One of the key advantages of  $\mu$ FIA is its ability to provide highly sensitive analysis, with detection limits in the nanomolar to picomolar range. This is due to the high surface-to-volume ratio of the microchannels, which allows for efficient mixing of the sample and reagent, as well as enhanced mass transfer between the phases. This makes  $\mu$ FIA a powerful tool for the analysis of trace-level analytes in complex matrices, such as environmental and biological samples. (Muhammad Rizwan Javed, 2018)

$\mu$ FIA has been successfully applied to a wide range of analytes, including pharmaceuticals, environmental contaminants, and biomolecules. For example,  $\mu$ FIA has been used for the detection of antibiotics in environmental samples (Silva, 2018),

the determination of amino acids in food products (Gonzalez, 2018), and the analysis of proteins in biological fluids. In each of these applications,  $\mu$ FIA provided rapid and sensitive analysis, with detection limits in the low nanomolar range.

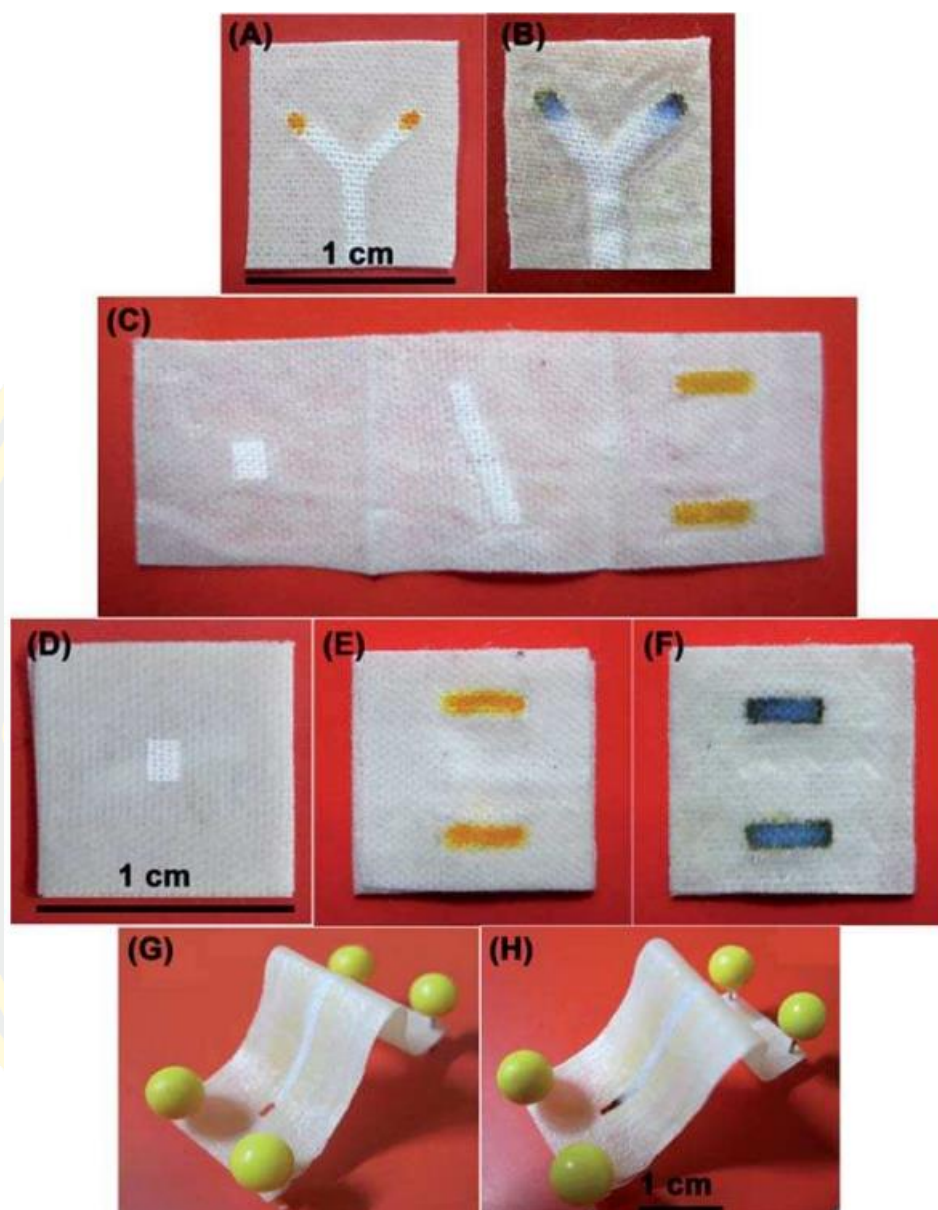
In addition to its high sensitivity,  $\mu$ FIA is also highly versatile, with the ability to be coupled with a wide range of detectors and separation techniques. For example,  $\mu$ FIA has been coupled with capillary electrophoresis (CE) for the separation and analysis of amino acids, and with liquid chromatography (LC) for the determination of pharmaceuticals in biological samples (Li, 2018). This versatility makes  $\mu$ FIA an attractive option for a wide range of applications in analytical chemistry.

In conclusion, microflow injection analysis is a powerful and versatile analytical technique that has gained popularity in recent years due to its high sensitivity, low cost, and ability to provide rapid and high-throughput analysis of samples. Its miniaturized nature allows for the analysis of trace-level analytes in complex matrices, making it an ideal tool for environmental, pharmaceutical, and biological applications.

### **2.3 Cloth-based analytical device; $\mu$ CAD**

Currently, the analysis and detection of substances, such as heavy metal contaminants in environmental samples, as well as biological indicators in liquid samples of living organisms for disease diagnosis, have become increasingly important. Usually, measurements and analyses are performed in a laboratory that requires the use of large and expensive equipment. Expertise is needed to analyze the samples, and the process is time-consuming and costly for each analysis. Microfluidic technology is a technology that deals with low-volume fluids ranging from nanoliters to microliters that flow in a channel (or at least in one dimension of the channel) with sizes ranging from micrometers to nanometers. (Jonathan S. Daniels, 2019) Currently, there has been a study and development of such technology as a new alternative for analyzing substances by reducing the size of the traditional analytical process into a small measurement device called a microfluidic device. The main goal of this type of measurement device is to enable all analysis steps to be performed on a single measurement device, using a small amount of sample and reagents, and be portable for on-site testing. It is also designed to be cost-effective. The materials commonly

used to create the measuring device are glass or plastic (Jane Doe, 2020). Recently, filter paper has gained a lot of interest as a material for creating measurement devices. These measurement devices are called paper-based microfluidic analytical devices. This type of measurement device has a production method that is not complicated, and the experimenter does not need to be an expert. The cost of production is low because filter paper is inexpensive, which is an important factor in making this measurement device widely used. It can be easily accessed, especially in developing countries (Ahmed, 2021). However, the use of paper as a material for device fabrication has limitations in detection. For example, paper can tear and degrade easily, and it is difficult to reuse. Recently, fabric has been used as a material for creating measurement devices, as an alternative in chemical analysis development. The fabric has properties that allow for good water absorption, is lightweight and thin, inexpensive, easy to obtain, highly flexible, and does not easily tear or wear out, making it suitable for creating testing devices. This type of measurement device is called a cloth-based analytical device or  $\mu$ CAD. The process of creating the cloth-based analytical device ( $\mu$ CAD) involves two main parts. First, a hydrophobic zone is created as a pattern on the fabric for testing purposes. Second, the hydrophilic zone (Chen, 2021) for testing is created using various techniques such as photolithography, polymer screen-printing method, wax screen-printing method, and others. These techniques allow for the creation of a testing area on the fabric that is water-loving and capable of performing the desired analysis. There are several methods for detection in the  $\mu$ CAD system, such as colorimetric detection and electrochemical detection.



Figures 2-2 Cloth-based analytical device for colorimetric detection. (Nilghaz et al., 2012)

## 2.4 Microfluidic Systems with Amperometric Detection

Microfluidics is a rapidly growing field that involves the manipulation and control of small volumes of fluids within microchannels. The integration of microfluidic systems with amperometric detection techniques has led to the

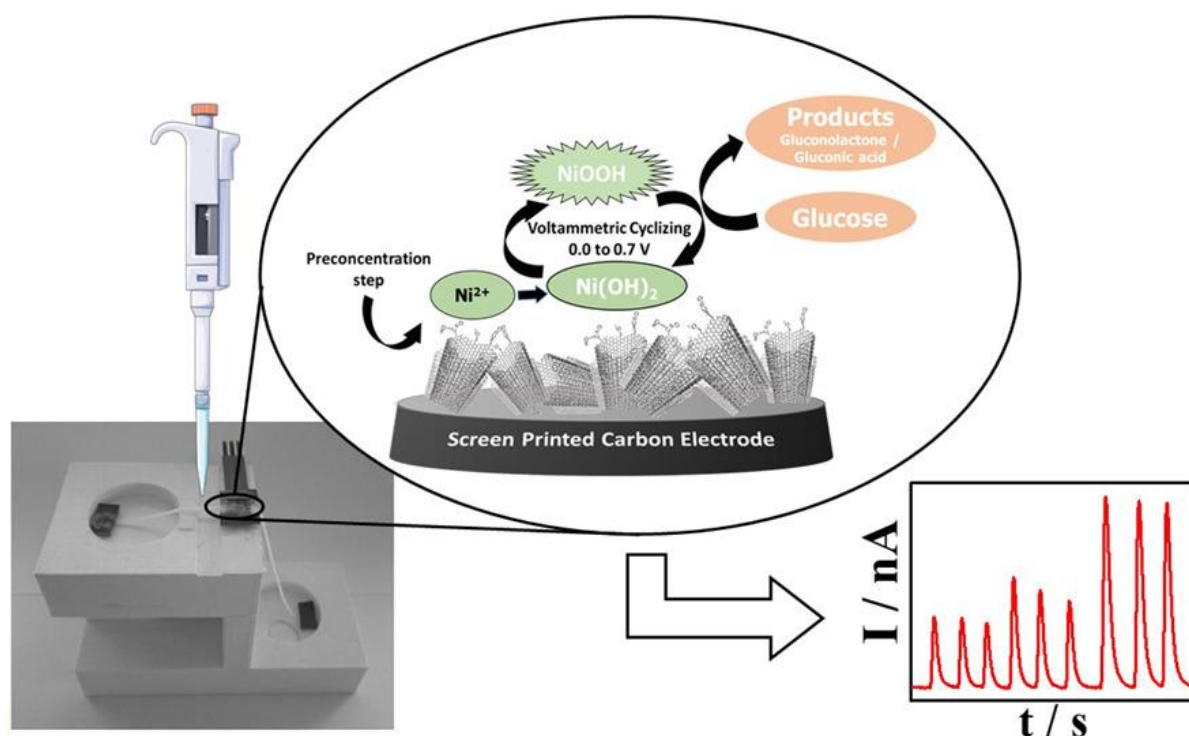
development of sensitive and reliable analytical devices for various applications such as biomedical, environmental monitoring, and food analysis.

Amperometric detection is a widely used electrochemical technique that measures the current produced by the oxidation or reduction of analytes. The integration of microfluidic devices with amperometric detection offers several advantages over traditional bulk measurements, including high sensitivity, rapid response time, and low sample consumption. Microfluidic systems with amperometric detection are particularly useful for the detection of low concentrations of analytes in complex matrices.

One of the significant advantages of microfluidic systems with amperometric detection is their high sensitivity. The miniaturization of electrodes in microfluidic devices leads to a significant increase in sensitivity compared to traditional bulk measurements. For example, in a recent study, a microfluidic device with a 3D-printed electrode was developed for the detection of glucose in blood samples. The device exhibited a sensitivity of  $8.44 \mu\text{A}/\text{mM}$  and a linear range of 0.1-10 mM, which is comparable to the sensitivity of commercial glucose sensors. (J. Wang et al., 2021)

In addition to high sensitivity, microfluidic systems with amperometric detection also offer a rapid response time. The small volume of the microchannels allows for faster diffusion of analytes towards the electrode surface, leading to a shorter response time compared to traditional bulk measurements. For example, a microfluidic device with a nanoporous gold electrode was developed for the detection of  $\text{H}_2\text{O}_2$ . The device exhibited a response time of less than 1 s, which is significantly faster than traditional bulk measurements. (Y. Wang, Zhu, Huang, Li, & Li, 2019)

Despite the numerous advantages of microfluidic systems with amperometric detection, there are still some limitations that need to be addressed. One of the significant limitations is the fabrication and integration of microfluidic devices with amperometric detection. The fabrication of microfluidic devices with precise channel geometries and electrode placement can be challenging and time-consuming. Moreover, the integration of amperometric detection with microfluidic systems requires careful optimization of electrode materials, geometries, and operation conditions to achieve reliable and reproducible results.



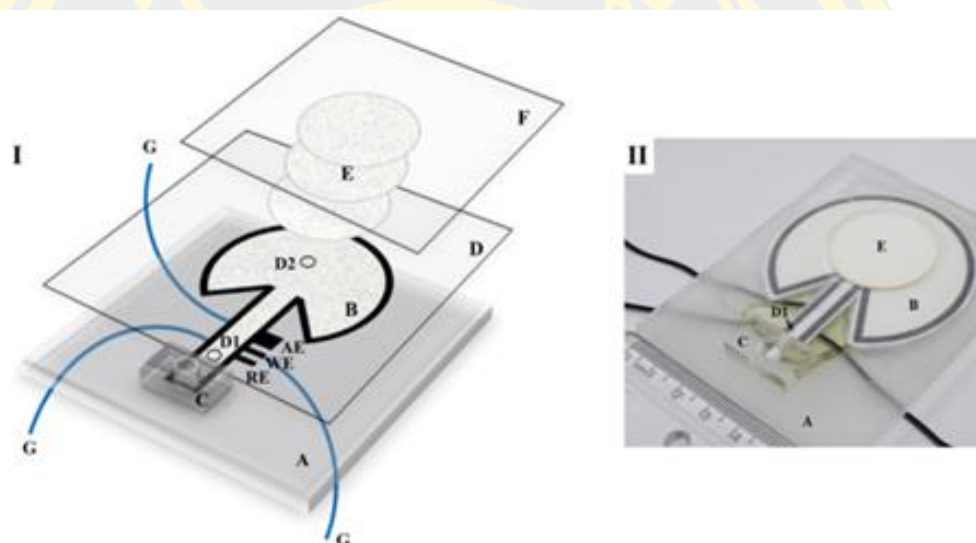
Figures 2-3 Microfluidic system of cotton thread Analyzed by amperometric technique. (Oliveira et al., 2019)

## 2.5 Related literature reviews

Pradela-Filho and coworkers (Pradela-Filho et al., 2020) reported an affordable and simple continuous flow electrochemical paper analytical device (CF-ePAD) coupled with a thermoplastic elastomer (TPE). The device has rapid and continuous flow when analyzing fluid injection, by adding two inlet reservoirs to a channel that utilizes the same paper and flows through an electrochemical detector. The process ends in a water-sucking reservoir. The inlet reservoirs are filled with buffer and allow continuous flow through the device. The sample injection was carried out by adding 2 microliters of the sample to the bottom inlet channel. The difference in flow resistance resulted in the sample plug changing the buffer when flowing through the working electrode.

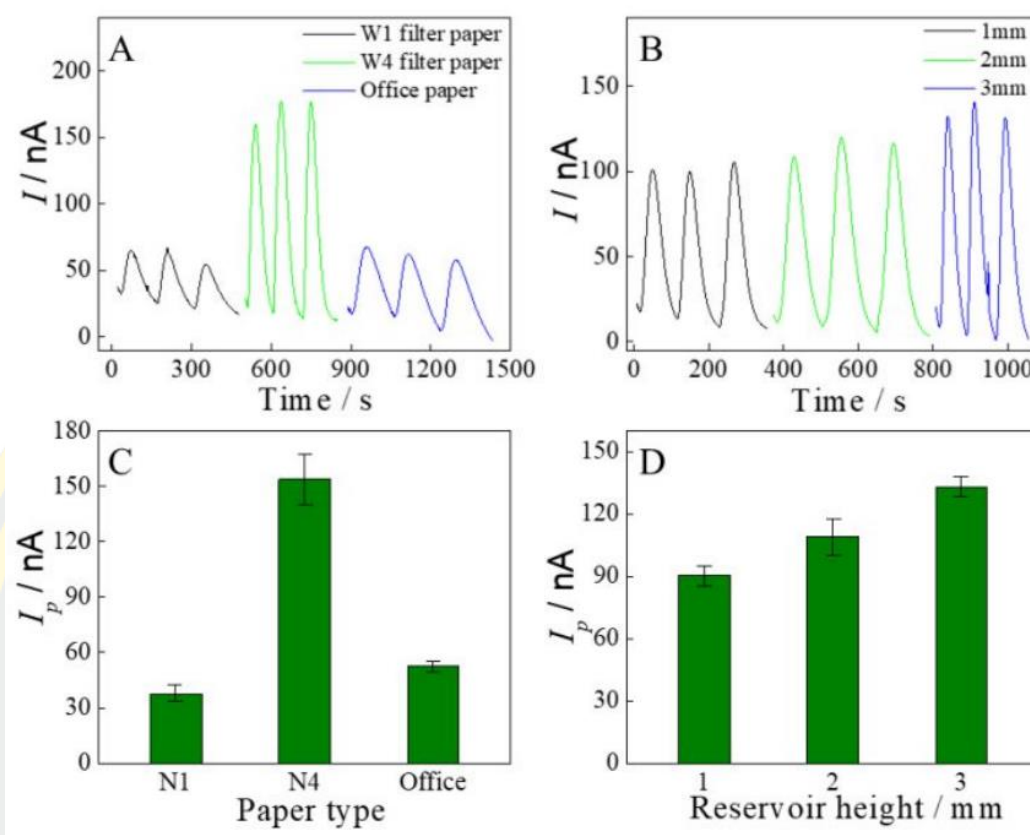
The electrochemical detector was created by mixing carbon black and polycaprolactone (50% w/w). The CF-TPE-ePADs have a distinctive feature of chronamperometry, using ferrocenylmethyltrimethylammonium as the electroactive

species. The appropriate flow rate and injection volume make analysis faster than previous reports of flow injection analysis. To demonstrate the use of CF-TPE-ePADs, the sensor was used to determine amount of caffeine in three different tea samples. The presented method has a linear range of 10 to 500  $\mu\text{mol L}^{-1}$  with detection and quantification limits of 2.5 and 8.3  $\mu\text{mol L}^{-1}$ , respectively. This approach shows potential in creating affordable and simple flow injection analytical devices without compromising efficiency.



Figures 2-4 (I) The schematic diagram of CF-TPE-ePAD. (II) shows the image of the CF-TPE-ePAD characteristics. (Pradela-Filho et al., 2020)

The signal of the FIA system can be observed (Figure 2-5) when the analysis substance flows into the microfluidic channel at a constant flow rate and is detected in the detection zone. Figure 2-5 also shows the influence of the paper surface on the amperometric signal.

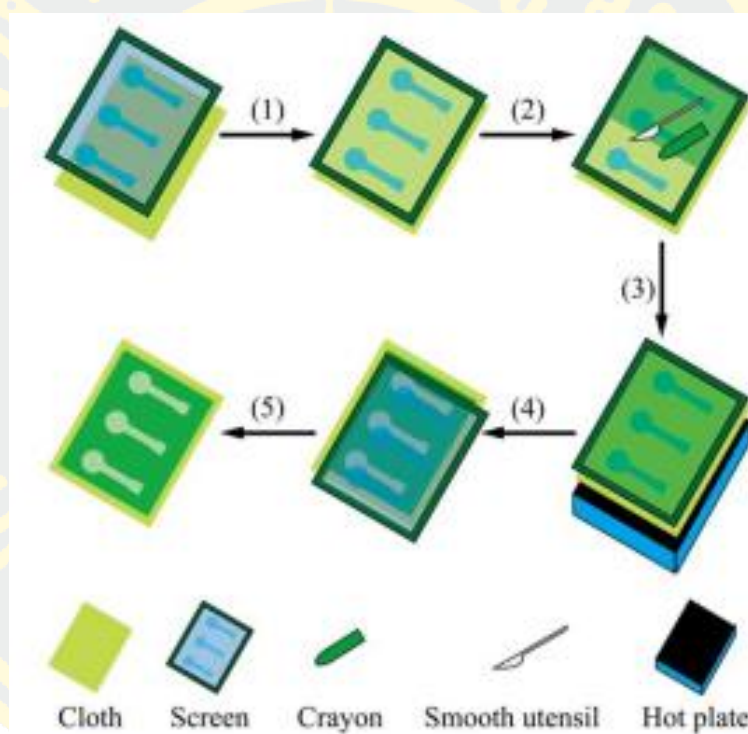


Figures 2-5 The influence of the paper substrate on the amperometric signal. (Pradela-Filho et al., 2020)

Wenrong Guan and coworkers (Guan, Zhang, Liu, & Liu, 2015) reported the chemiluminescence (CL) detection for microfluidic analysis devices using microfiber-coupled analysis device ( $\mu$ CAD). The device was created using wax screen-printing method to create channels or test zones on the fabric as shown in Figure 2-6. Firstly, the screen was placed on the fabric (Step 1) and then coated with green-colored emulsion to increase the amount of wax filling in the fabric for the next screen-printing process (Step 2). Then, the fabric was placed on a hot plate with a mesh and heated for approximately 5 seconds at 85 °C to melt the wax into the fabric to create a hydrophobic barrier (Step 3). After that, the mesh and fabric were removed from the hot plate (Step 4). Finally, the wax-patterned fabric was ready for use (Step 5).

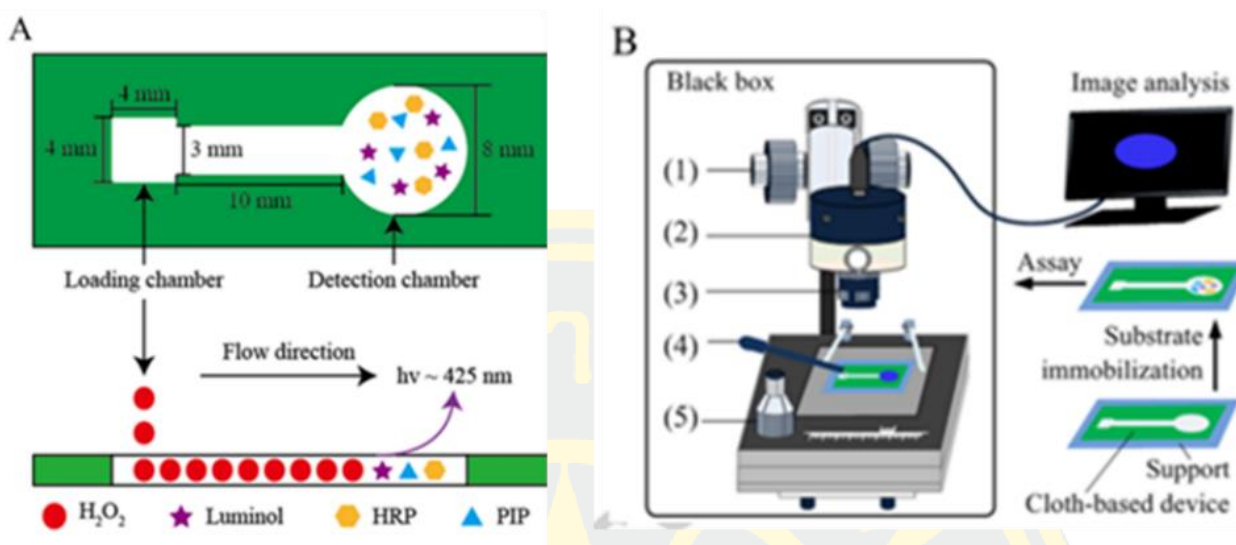
The CL assay was employed to demonstrate the applicability of the developed device. The analysis of  $\text{H}_2\text{O}_2$  is carried out using the enzyme assay where

the luminol, HRP and PIP were immobilized on the detection zones. Upon the reaction with the reagents, the chemiluminescence signal produced and then imaged using a low-cost CCD camera. A linear correlation between the CL intensity and the  $\text{H}_2\text{O}_2$  concentration in the range of 0.5-5 mM was obtained with a detection limit of 0.46 mM. Finally, the usefulness of the fabric-based CL device was demonstrated in the detection of  $\text{H}_2\text{O}_2$  residue in animal tissue samples. Chicken meat soaked in 3%  $\text{H}_2\text{O}_2$  for 6 hours was detected. Furthermore, the excess ground meat samples can be directly used without the need for additional processing.



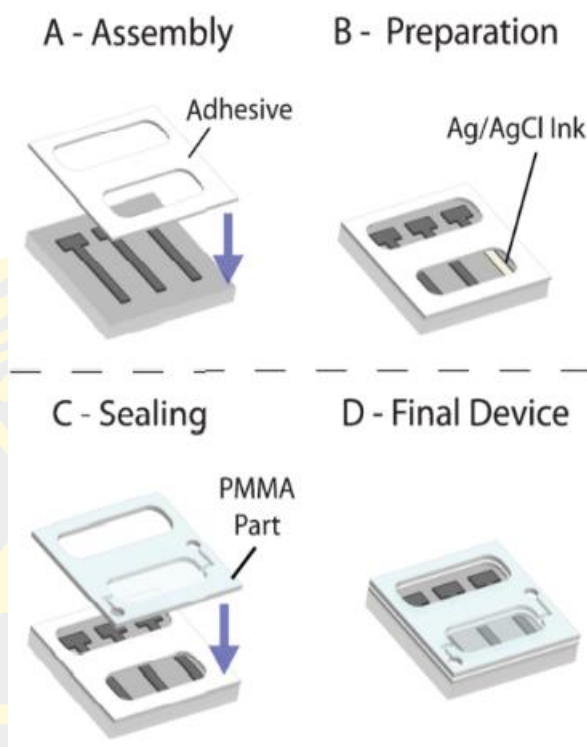
Figures 2-6 Schematic illustration of wax-screen-printing for fabrication of  $\mu\text{CADs}$ .

(1) The screen is placed over the cloth; (2) the screen is rubbed with a crayon and smooth utensil; (3) the cloth is placed on the heating board together with the screen; (4) the screen and cloth are removed from the heating board; (5) the patterned cloth is separated from the screen. (Guan et al., 2015)



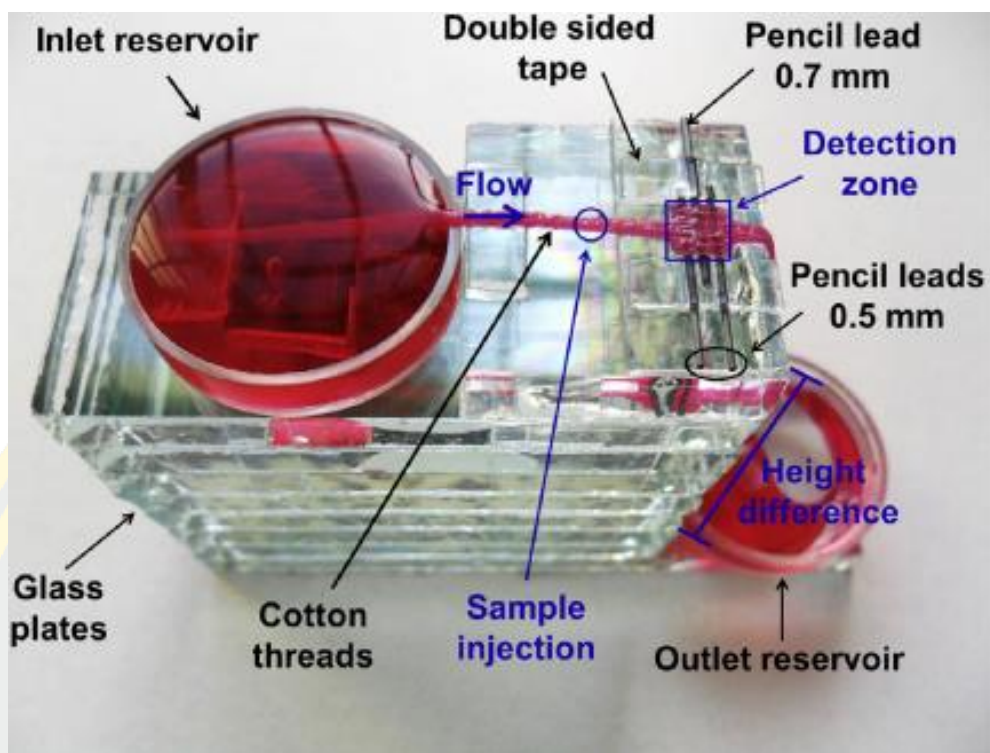
Figures 2-7(A) The characteristics of a fabric-based device used for the analysis of  $\text{H}_2\text{O}_2$  through chemiluminescence detection. The size of the detection area and the quantification of  $\text{H}_2\text{O}_2$  on the fabric-based device are shown. (B) shows the detection and analysis of microfluidic chemiluminescence on the fabric-based device. (Guan et al., 2015)

Neus Godino and coworkers (Godino, Gorkin, Bourke, & Ducree, 2012) developed an electrical chemical sensing device using disposable materials such as paper and polymer. A paper-based device was created by printing a bee wax pattern onto the paper surface using a wax printing method, followed by the creation of a carbon electrode on the paper using a screen printing or stencil printing technique. The electrode was then dried at  $70^\circ\text{C}$  for 30 minutes. The paper was coated with a polymer layer, sealed with a pressure-sensitive adhesive (PSA) layer, and the reference electrode was attached with a drop of silver/silver chloride. The assembled device was dried at  $70^\circ\text{C}$  for 30 minutes, resulting in a paper and polymer-based device with a high-performance electrical chemical sensor suitable for field use.



Figures 2-8 Steps for assembling the wax-carbon electrode printed on paper and polymer substrate. (Godino et al., 2012)

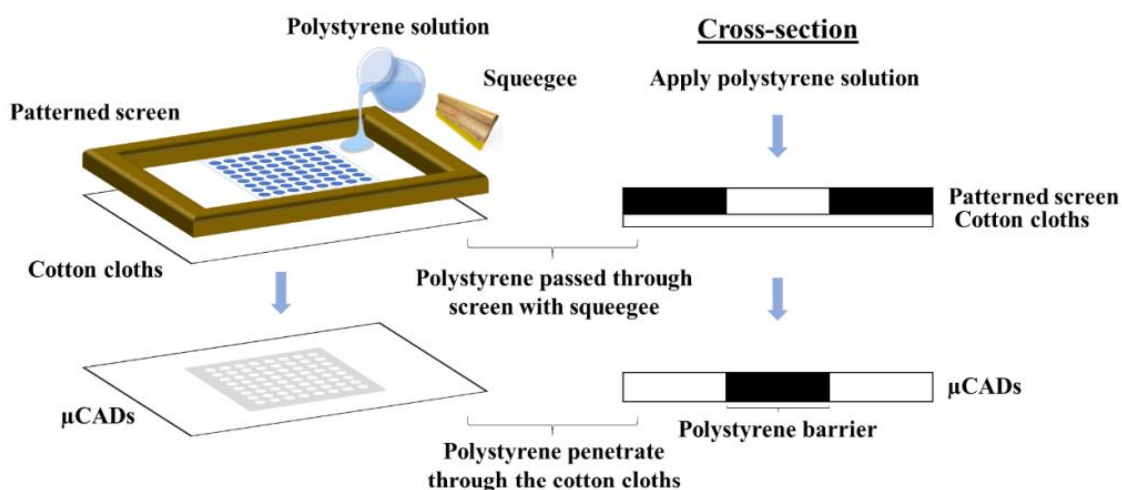
Deonir Agustini and coworkers (Agustini et al., 2016) developed microflow injection analysis ( $\mu$ FIA) system using a microfluidic channel on a thread for simple and low-cost production. In this analysis, the solvent flows through the thread using capillary and gravitational forces without the need for external pumps. The supporting electrolyte flows from the top inlet reservoir through the injection area, detection area, and down to the bottom outlet reservoir, using a graphite electrode as a working electrode. The system was tested by detecting naproxen (NPX) as a standard compound using chronoamperometric analysis. The detection limit was found to be  $0.29 \text{ mmol L}^{-1}$  with a relative standard deviation (%RSD) of 1.69%.



Figures 2-9 Microfluidic system on a fabric-based device for electrochemical detection. (Agustini et al., 2016)

Benjarat Tasaengtong and coworkers (Tasaengtong & Sameenoi, 2020a) developed a simple and low-cost screen printing method for the production of microfluidic cloth-based analytical devices ( $\mu$ CAD). The method uses polystyrene and a screen block, with the process of creating a test area on fabric by allowing the polystyrene solvent to pass through the screen block pattern and penetrate the cotton fabric to create a hydrophobic region. In this research, various cotton fabrics and polystyrene concentrations were studied. The cotton fabrics were cleaned with hot water,  $\text{Na}_2\text{CO}_3$  solution, and  $\text{NaOH}$  solution to improve the water absorption ability of the fabric. It was found that the highest absorption rate was achieved by using  $\text{Na}_2\text{CO}_3$  followed by  $\text{NaOH}$  for cleaning the fabric in hot water and untreated fabric in the most suitable condition for the smallest hydrophilic and hydrophobic areas were  $678 \pm 59 \mu\text{m}$  and  $329 \pm 27 \mu\text{m}$ , respectively. The reproducibility of the devices was determined by measuring the standard deviation of the central line passing through the test area of the circular device designed with a 5 mm and 7 mm diameter, resulting in

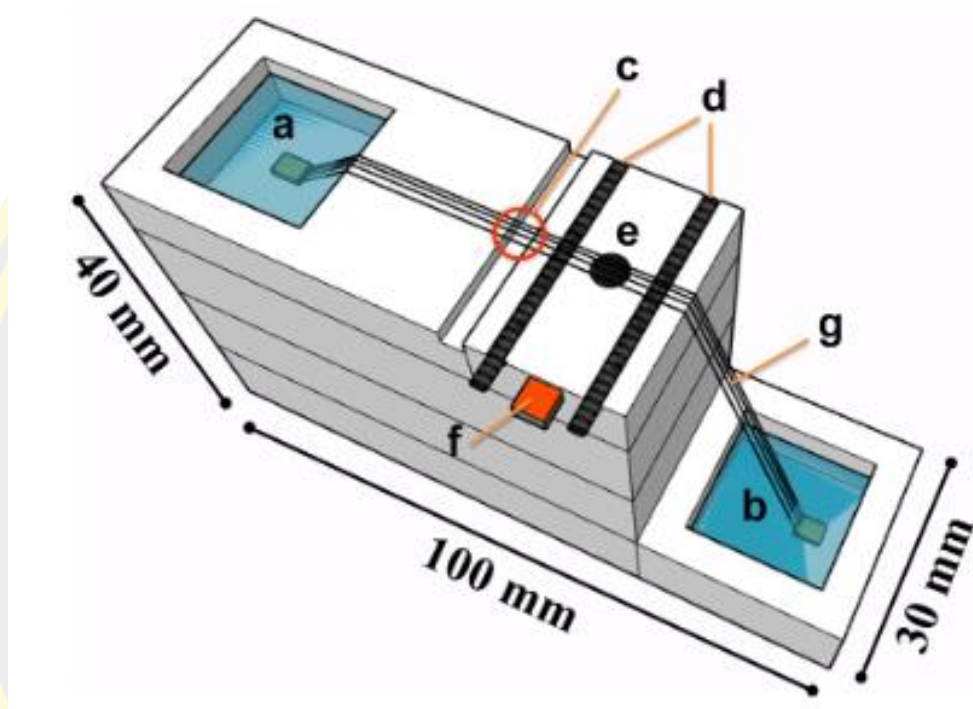
a standard deviation of 1.1-2.0% (n=64). Various device designs can be created in  $\mu$ CAD by adjusting the screen pattern to fit with different organic solvents.



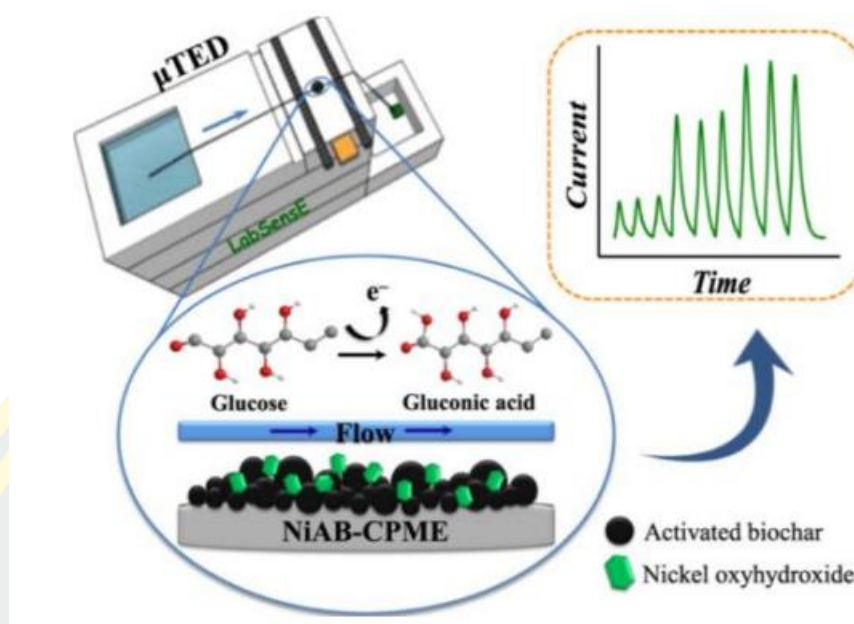
Figures 2-10 A one-step screen printing method using polymer for the fabrication of microfluidic analysis devices with a microfiber cloth ( $\mu$ CADs). (Tasaengtong & Sameenoi, 2020a)

Cristiane Kalinke and coworkers (Kalinke et al., 2019) reported the use of a nickel-based carbon paste-modified electrode (NiAB-CPME) coupled with a microfluidic thread-based electrochemical detection ( $\mu$ TED) for non-enzyme-catalyzed glucose sensing. The microfluidic device was assembled on a plastic substrate using 3D printing technology, which is easy to construct using low-cost materials. The device employed an amperometric glucose sensor without the use of enzymes in  $\mu$ TED, demonstrating good reproducibility of 3.84% for continuous glucose injection (n=10), a steady flow rate of  $1.11 \mu\text{L s}^{-1}$ , and an analysis frequency of 61 injections per hour in a linear dynamic range (LDR) of 5.0 to  $100.0 \mu\text{mol L}^{-1}$ . The limit of detection (LOD) was  $0.137 \mu\text{mol L}^{-1}$ , and the limit of quantitation (LOQ) was  $0.457 \mu\text{mol L}^{-1}$  for glucose. Thus, the activated NiAB-CPME can be used as an alternative platform to use as a non-enzyme electrochemical sensor for measuring

blood sugar levels. An amperometric detection-based sensor was employed in a microfluidic device to develop a green method for glucose determination in biological fluids (human serum and saliva).



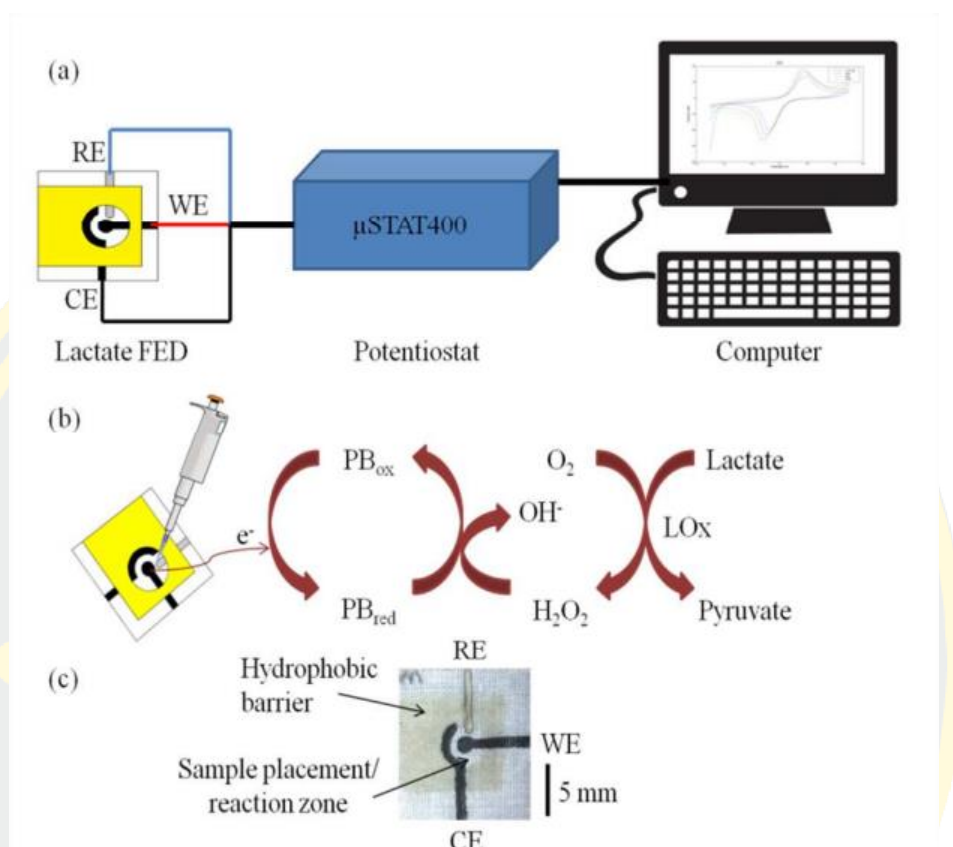
Figures 2-11 Construction of  $\mu$ TED with an inlet (a) and outlet reservoirs (b), injection zone (c), cavities for the accommodation of auxiliary and reference electrodes of cylindrical graphites (d), orifice for carbon paste accommodation (work electrode) (e) with a copper electrical contact (f) and textile threads (g). (Kalinke et al., 2019)



Figures 2-12 The Microfiber-based Electrochemical Detection Device ( $\mu$ TED) and its application in detection and measurement are reported in this article. (Kalinke et al., 2019)

Radha S. P. Malon and coworkers (Radha S.P. Malon, K.Y. Chua, Wicaksono, & Córcoles, 2012) described a method for the determination of lactate concentration in saliva samples by using a simple and low-cost cotton fabric-based electrochemical device (FED). The device was fabricated using template method for patterning the electrodes and wax-patterning technique for creating the sample placement/reaction zone. Lactate oxidase (LOx) enzyme was immobilized at the reaction zone using a simple entrapment method. The LOx enzymatic reaction product, hydrogen peroxide ( $\text{H}_2\text{O}_2$ ) was measured using chronoamperometric measurements at the optimal detection potential ( $-0.2$  V vs. Ag/AgCl), in which the device exhibited linear working range between 0.1 to 5 mM, sensitivity (slope of  $0.3169 \mu\text{A mM}^{-1}$ ) and detection limit of 0.3 mM. The low detection limit and wide linear range were suitable to measure salivary lactate (SL) concentration, thus saliva samples obtained under fasting conditions and after meals were evaluated using the FED. The measured SL varied among subjects and increased after meals randomly. The proposed device provides a suitable analytical alternative for rapid and non-invasive determination of lactate in

saliva samples. The device can also be adapted to a variety of other assays that requires simplicity, low-cost, portability and flexibility.



Figures 2-13 Overview of FED technology. (a) The instrumental setup for lactate determination. (b) The reaction that occurs at the C-PB/LOx electrodes of the FED. (c) Picture of the fabricated FED (15 x 15 mm). RE, reference electrode; WE, working electrode; CE, counter electrode. (Radha S.P. Malon et al., 2012)

## CHAPTER 3

### EXPERIMENTAL

#### 3.1 Materials and chemicals

##### 3.1.1 Materials

1. Analytical Balance 4 Digits, Model MS, Mettler Toledo
2. Analytical Balance 2 Digits, Model PL-E, Mettler Toledo
3. Oven, Model 1375 FX, Delta Laboratory Co., Ltd., Thailand
4. Magnetic stirrer, model C-MAG HS 7, IKA Works (Thailand) Co. Ltd., Thailand
5. Micropipette, model Eppendorf Research, Eppendorf
6. Potentiostat, Model  $\mu$ Stat400, Brand DropSens
7. pH meter, Model Starter 3100, OHAUS
8. Block screen made to order from the block screen shop, Nong Mon market, Chonburi, Thailand
9. PVC patterned film (made by crafted using a Silhouette Cameo Model 1, Silhouette America, USA)
10. Cotton, pan muslin brand, local market, Chonburi, Thailand
11. Ultrasonic cleaner, model Elmasonic S30H, Elma Electronic Co., Ltd.
12. Clear masking tape, model 3M, Scotch, Thailand
13. Double-sided adhesive tape, thin type, Q-BIZ International Co., Ltd.
14. Hot magnet stirrer (C-MAG), Germany
15. HUCO Hot Melt Glue Gun, Model TG-03 Power 120 - 240 V. 10 W. Black, China
16. Oil paint, Silpakorn Pradit brand, green color, Thailand
17. Syringe Filter, Nylon type, pore size 0.45 micrometers, Therma Scientific™, Thailand

##### 3.1.2 Chemicals

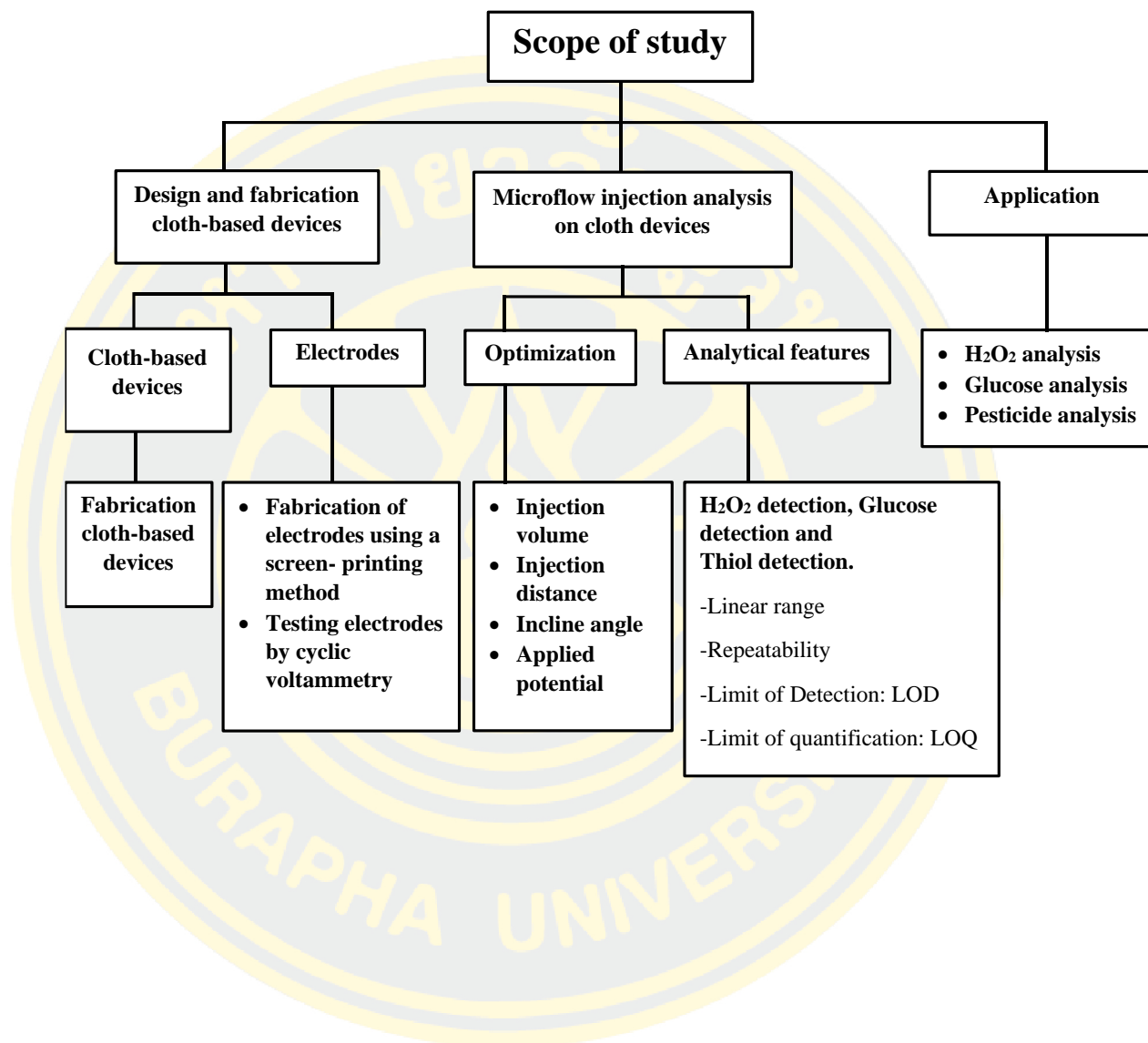
1. Toluene, (C<sub>6</sub>H<sub>5</sub>CH<sub>3</sub>) CAS Number: 108-88-3, Commercial grade, RCI Labscan Thailand Co., Ltd.
2. Polystyrene (Foam), Stationery Store, Chonburi, Thailand

3. Prussian blue, ( $C_{18}Fe_7N_{18}$ ) CAS Number: 14038-43-8, Sigma Aldrich, USA
4. Ag/AgCl paste, Sun Chemical, England
5. Hydrogen peroxide, 35% ( $H_2O_2$ ) CAS Number: 7722-84-1, Commercial grade, Merck KGaA, Germany
6. Potassium nitrate, ( $KNO_3$ ) CAS Number: 7757-79-1, AR grade, Ajax Finechem, Australia
7. Carbon graphite paste, Sun Chemical, England
8. Sodium carbonate, ( $Na_2CO_3$ ) CAS Number: 497-19-8, Merck KGaA, Germany
9. Acetone, ( $CH_3COCH_3$ ) CAS Number: 67-64-1, Commercial grade, RCI Labscan Thailand Co., Ltd.
10. Tris (hydroxymethyl) aminomethane, CAS Number: 77-86-1
11. Acetyl Thiocholine Iodine ( $C_7H_{16}INOS$ ; ATCI) MW: 289.18 g/mol, CAS: 1866-15-5, Analytical Grade (Acros Organics, Belgium)
12. Bovine Serum Albumin, CAS Number: 9048-46-8, Calbiochem, USA
13. Acetylcholinesterase (AChE), CAS Number: 9000-18-1, EC 3.1.1.7 518 U/mg Solid and 3.9 mg solid, Sigma Aldrich, USA
14. Hydrochloric acid, HCl CAS Number: 7647-01-0, RCI Labscan Thailand Co.,Ltd.
15. Pesticide standard Chlorpyrifos-oxon, CPO CAS Number: 5598-15-2, MW. : 334.52 g/mol, Sigma Aldrich, USA
16. DL-dithiothreitol, ( $C_4H_{10}O_2S_2$ ) CAS: 3483-12-3, MW: 154.25 g/mol, AR grade, Sigma Aldrich, USA
17. D(+)-Glucose, ( $C_6H_{12}O_6$ ) CAS Number: 50-99-7, Merck KGaA, Germany
18. Glucose Oxidase (GOx), CAS: 9001 -37 -0, 117200 units/g solid, Sigma Aldrich, USA

### **3.1.3 Real samples**

Chicken feet samples were obtained from local market, Chonburi. Rice field water samples were collected from rice fields in Chonburi province area. Control serum samples were obtained from Human GmbH, Germany.

### 3.2 Research plan



### 3.3 Preparation of solutions

#### 3.3.1 *Polystyrene solution 35% (w/v)*

A 7 g of polystyrene was dissolved in 20 mL of toluene and mixed with 2 drops of the paint. The mixture solution was degassed for 15 min to get rid of the air bubbles prior to use as a hydrophobic material to fabricate the cloth-based microflow system.

#### 3.3.2 *Sodium carbonate (Na<sub>2</sub>CO<sub>3</sub>) solution*

A 1% (w/v) sodium carbonate solution was prepared by dissolving 3.0 g of sodium carbonate in 300 mL deionized water.

#### 3.3.3 *Electrodes containing carbon paste 0.8 g and Prussian blue 0.2 g*

A homogeneous paste was obtained by mixing 0.8 g of carbon paste with 0.2 g of Prussian blue and used as a material to fabricate working electrodes.

#### 3.3.4 *Potassium nitrate solution*

Potassium nitrate solution (1 M) was prepared by dissolving 10.1100 g of KNO<sub>3</sub> in deionized water and the solution made up to 100 mL using deionized water. This solution acted as a supporting electrolyte and a carrier solution of the flow system.

#### 3.3.5 *Hydrogen peroxide solution*

Stock H<sub>2</sub>O<sub>2</sub> solution (1 M) was prepared by pipetting 430  $\mu$ L of 35% H<sub>2</sub>O<sub>2</sub> solution (11.63 M) into a 5 mL volumetric flask and the solution was made up to the volume using deionized water. This solution was used to prepare a working H<sub>2</sub>O<sub>2</sub> solution with a concentration of 0.5-12.5 mM in 1 M KNO<sub>3</sub> solution.

#### 3.3.6 *Hydrochloric acid solution*

Hydrochloric acid solution (1 M) by pipetting 828  $\mu$ L 37% HCl solution (12.08 M) by into a beaker containing 9.17 mL of deionized water. Then, the solution is mixed until homogeneous.

#### 3.3.7 *Tris buffer solution pH 7.4*

Tris buffer solution (10 mM) was prepared by weighing 0.1211 g Tris (hydroxymethyl) aminomethane into a small beaker and dissolving using deionized water. Then, the solution was transferred into a 100 mL volumetric flask and the volume adjusted using deionized water. The pH of the solution was measured using a pH meter and adjusted to the desired pH using 1 M HCl solution.

### **3.3.8 Bovine serum albumin; BSA in Tris buffer solution**

Bovine serum albumin solution was prepared by dissolving 100 mg of Bovine serum albumin in 10 mL Tris buffer pH 7.4. The solution was mixed until homogeneous.

### **3.3.9 Acetylthiocholine solution**

Acetylthiocholine solution (5 mM) was prepared by dissolving 2.9 mg of ATC in deionized water and the final volume was made up to 2 mL with deionized water.

### **3.3.10 Acetylcholinesterase Enzyme (AChE)**

A 1000 U/mL stock solution of acetylcholinesterase (AChE) was prepared by dissolving 3.9 mg solids (518 U/mg solids) of AChE in 2000  $\mu$ L phosphate buffer pH 7.4 and stored at -20 °C until use.

A 2 U/mL AChE solution was prepared by diluting the 1000 U/mL stock solution of AChE with BSA solution (section 3.3.8) and stored at -20 °C until use.

### **3.3.11 Pesticide standard Chlorpyrifos-oxon (CPO)**

A solution of 10-100 ng/mL chlorpyrifos-oxon (CPO) was prepared by diluting the stock solution of 1000 ng/mL CPO using 4% (v/v) methanol and storing at 2-8 °C until use.

### **3.3.12 Dithiothreitol solution (DTT)**

Dithiothreitol (DTT) solution (50 mM) was prepared by weighing 7.71 mg of DTT into a small beaker dissolved in deionized water. This solution was used to prepare a working dithiothreitol solution with a concentration of 1-10 mM in 1 M KNO<sub>3</sub> solution.

### **3.3.13 Glucose solution**

Glucose solution (50 mM) was prepared by weighing 9 mg of D(+)-Glucose into a small beaker dissolved in deionized water. This solution was used to prepare a working glucose solution with a concentration of 0.5-15 mM in deionized water.

### **3.3.14 Bovine serum albumin; BSA in 0.1 M phosphate buffer solution pH 7**

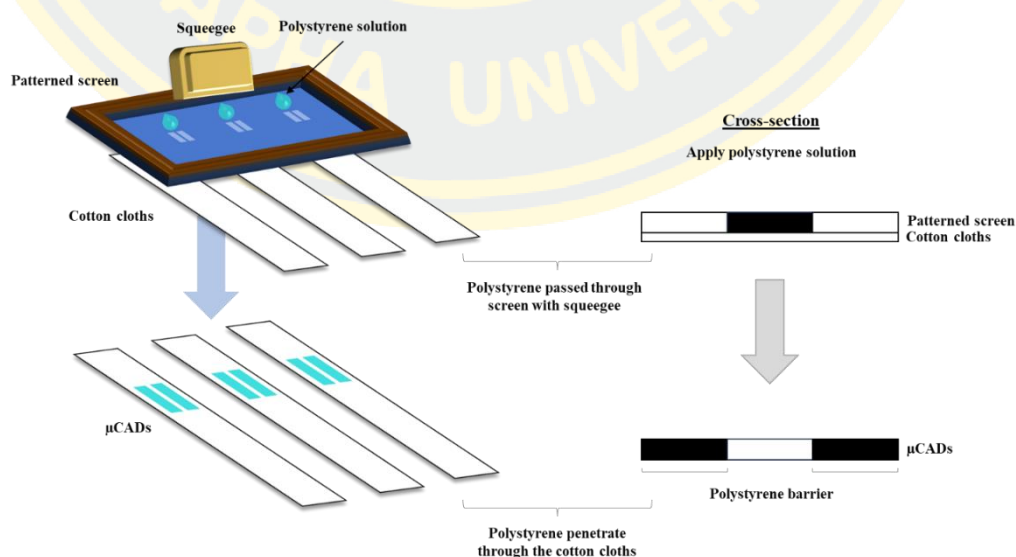
Bovine serum albumin solution was prepared by dissolving 1 mg of Bovine serum albumin in 1000  $\mu$ L 0.1 M phosphate buffer solution pH 7. The solution was mixed until homogeneous.

### 3.3.15 Glucose Oxidase (Gox)

Glucose oxidase (150 U/mL) was prepared by diluting a 25,000 U/mL stock solution of glucose oxidase with BSA in 0.1 M phosphate buffer solution pH 7 (from clause 3.3.14) and the aliquot stored at -20 °C until use.

## 3.4 Design and fabrication of cloth-based devices.

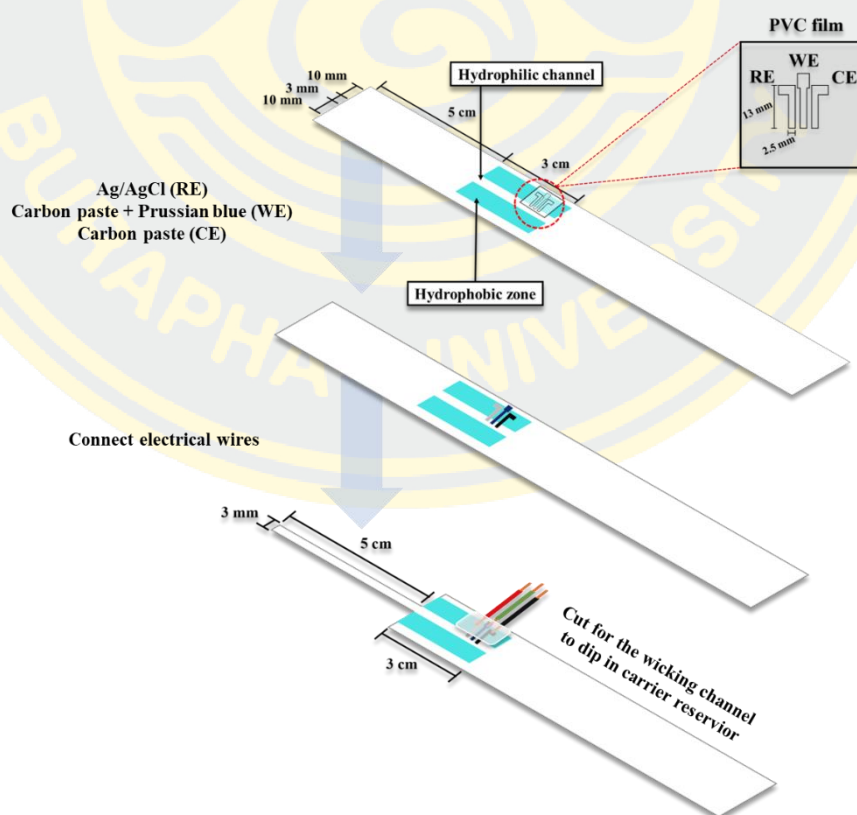
The microflow system on cloth was fabricated using a one-step polymer screen-printing method. (Tasaengtong & Sameenoi, 2020b) The process began with scouring the cotton cloth to remove the dirt by immersing it in Na<sub>2</sub>CO<sub>3</sub>. The solution was heated at 100 °C for 5 min. The cloth was then removed and rinsed with water and allowed to dry at room temperature. The cloth was cut to have a width of 15 mm and a length of 35 cm. A screen of the desired pattern to create a channel with a dimension of 0.3 cm wide and 3 cm long was placed on a cloth. The prepared polystyrene solution (35% w/v in toluene) was poured and squeegeed onto the screen to allow the solution to penetrate through the screen and to the bottom of the cloth in Figure 3-1. The screen was removed and the cloth was allowed to dry to create a hydrophobic barrier and a channel to allow for the solution flow. The back side of the fabricated cloth was adhered with clear packing tape to prevent leakage of the solution during the experiment.



Figures 3-1 Procedure for Fabrication of the  $\mu$ CAD using the polymer screen printing method.

### 3.5 Fabrication of electrodes using stencil transparent film-printing method on cloth ( $\mu$ CAD)

The electrodes were fabricated at the end of the device using stencil transparent film-printing method. The procedure begins with creating the patterned stencil PVC film. The stencil lamination film was placed over the channel of the cloth-based device and the electrode materials were squeegeed over the patterned film where the silver-silver chloride, bare carbon paste and carbon paste mixed with Prussian blue (20% wt) were used as reference (RE), auxiliary (AE) and working electrodes (WE), respectively (Figure 3-2). The cloth-based device containing electrodes was then dried at 45°C for 10 min and the copper wires connected using with silver ink as a connector and baked at 45°C for another hour. Finally, cloth at the front end of the devices was cut to have a hydrophilic channel with the dimension of 3 mm wide and 5 cm long and was used to dip into the carrier solution for the flow system.



Figures 3-2 Procedure for electrode fabrication using stencil lamination film printing.

### 3.6 Electrochemical characterization on cloth-based devices by cyclic voltammetry

The electrodes fabricated on the cloth-based device was tested for the performance using the cyclic voltammetry. The experiment was performed with the static condition where the  $\mu$ CAD in the zone containing the electrochemical detection zone was cut and the  $\text{KNO}_3$  electrolyte was dropped onto the electrode using Dropsens potentiostat and DropView 8400 software. The conditions used to test the electrodes by the cyclic voltammetry technique are as follows:

Supporting electrolyte: 1.0 M  $\text{KNO}_3$

Detection potential: -1.2 V – 1 V

Scan rate: varied from 5-50 mV/s



Figures 3-3 Cyclic voltammetry measurement of the electrodes on the cloth-based devices.

### 3.7 Microflow injection analysis on cloth devices

The continuous microflow injection analysis system using the fabricated  $\mu$ CADs was constructed as shown in Figure 3-4. The hydrophilic cloth at the front end of the device was immersed in the carrier solution in the upper reservoir (1.0 M  $\text{KNO}_3$ ). The other end of the devices was immersed in the lower reservoir (waste

reservoir). The flow channel containing the electrode was tilted at an angle of 45 degrees to the plane to allow flow from the upper reservoir to the lower reservoir by both capillary and gravitational forces. The electrode was connected to the potentiostat using the wire connection. The analysis was carried out by injecting 3  $\mu\text{L}$  sample solution using pipette at the sample injection zone which was located at the 1.0 cm away from the reference electrode. The carrier solution flowed and pushed the sample to flow through the electrode and to the waste reservoir. The amperometric detection was recorded for the flow profile where the detection potential was -0.3 V and +0.3 V vs Ag/AgCl paste for were applied for detection of  $\text{H}_2\text{O}_2$  and pesticide, respectively. The conditions used in the experiment are as follows:

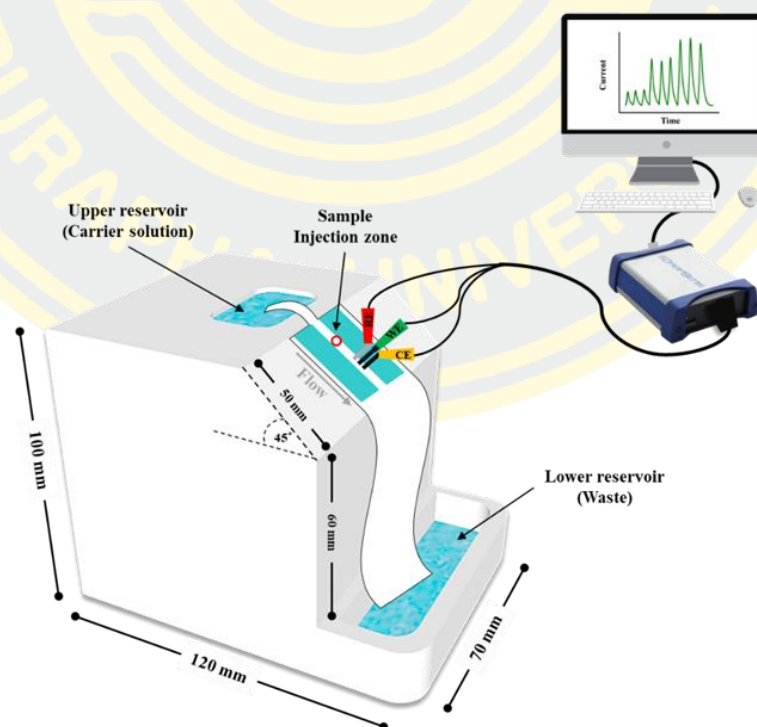
Supporting electrolyte: 1.0 M  $\text{KNO}_3$

Applied potential: -0.3 V vs. Ag/AgCl paste for  $\text{H}_2\text{O}_2$  and glucose and +0.3 V for pesticide detections

Injection volume: 3  $\mu\text{L}$

Injection distance (from reference electrode): 1.0 cm

Incline angle: 45°



Figures 3-4 Microflow system for continuous-flow electrochemical cloth-based microfluidic analytical devices (CF-e $\mu$ CADs).

### ***3.7.1 Optimum conditions analysis with microflow injection analysis***

#### ***3.7.1.1 Optimum injection volume of sample solution***

A solution of hydrogen peroxide ( $\text{H}_2\text{O}_2$ ) at a concentration of 1 mM with injection volumes of 1, 2, 3, and 4  $\mu\text{L}$  was evaluated to determine the optimal injection volume ( $n=3$ ). The default incline angle was set at 35 degrees, while other experimental conditions remained consistent with those outlined in section 3.7. Then, peak height ( $\mu\text{A}$ ), and peak area were plotted against the injection volume ( $\mu\text{L}$ ) to determine the appropriate injection volume.

#### ***3.7.1.2 Optimum injection distance of sample solution***

The injection distance of the sample, measured from the reference electrode and ranging from 0.4 to 1.2 cm, was examined to assess the optimal injection distance using a 1 mM  $\text{H}_2\text{O}_2$  solution with a 2  $\mu\text{L}$  injection volume. The default incline angle was maintained at 35 degrees, with all other experimental conditions remaining consistent with those detailed in section 3.7. Then, peak height ( $\mu\text{A}$ ), and peak area were plotted against the injection distance (cm) to inspect the appropriate injection distance.

#### ***3.7.1.3 Optimum Incline angle electrode area of the cloth-based device***

The inclination angle of cloth-based devices, aimed at facilitating rapid flow, was examined at angles of 20, 35, 45, and 50 degrees. A volume of 3  $\mu\text{L}$  of a 1 mM  $\text{H}_2\text{O}_2$  solution was injected into the system. All other parameters remained consistent with those outlined in section 3.7. Subsequently, peak height ( $\mu\text{A}$ ), and peak area were plotted against the inclination angle (degrees) to identify the optimal value.

## **3.8 Application of the developed microflow system**

### ***3.8.1 Hydrogen peroxide detection***

#### ***3.8.1.1 Applied potential***

The optimal applied potential for  $\text{H}_2\text{O}_2$  detection, within the range of +0 to -0.6 V, was assessed using hydrodynamic voltammetry by injecting 3  $\mu\text{L}$  1 mM  $\text{H}_2\text{O}_2$  solution into the flow system. All other experimental conditions remained consistent with the parameters described in section 3.7. The signal-to-baseline ratio (S/B) was

plotted as a function of applied potential to determine the appropriate potential and used for further experiments.

### ***3.8.1.2 Analysis of H<sub>2</sub>O<sub>2</sub> using the CF- $\mu$ CAD system***

H<sub>2</sub>O<sub>2</sub> analysis using the developed system was carried out. Different concentration of H<sub>2</sub>O<sub>2</sub> standard was prepared in the 1 M KNO<sub>3</sub> and injected into the system using the process described above. To further demonstrate the applicability in real samples, the analysis of H<sub>2</sub>O<sub>2</sub> in raw chicken feet was carried out. Firstly, the chicken feet were finely chopped and 3 g was soaked in 30 mL of deionized water for 20 min. The supernatant was filtered through a pore size 0.45-micron membrane using a nylon syringe filter (Therma Scientific™). The extracted solution was then analyzed using the developed system described above.

### ***3.8.2 Glucose detection***

The analysis of glucose was carried out by adding 20  $\mu$ L of 150 U/mL Glucose Oxidase (GOx) solution to a microtube. Next, a 20  $\mu$ L of glucose solution at concentrations ranging from 0.5 to 15 mM was added to the Gox solution. The solution was thoroughly mixed using a stirrer and allowed to react for 5 min to generate H<sub>2</sub>O<sub>2</sub> (follow in equation 2). Finally, the solution was measured using the developed CF- $\mu$ CAD system. For real sample analysis, the serum sample including HumaTrol N (normal range) and HumaTrol P (abnormal range) were employed and the assay were performed in similar manner to the procedure for glucose standard detection.



### ***3.8.3 Organophosphate pesticide detection***

#### ***3.8.3.1 Applied potential***

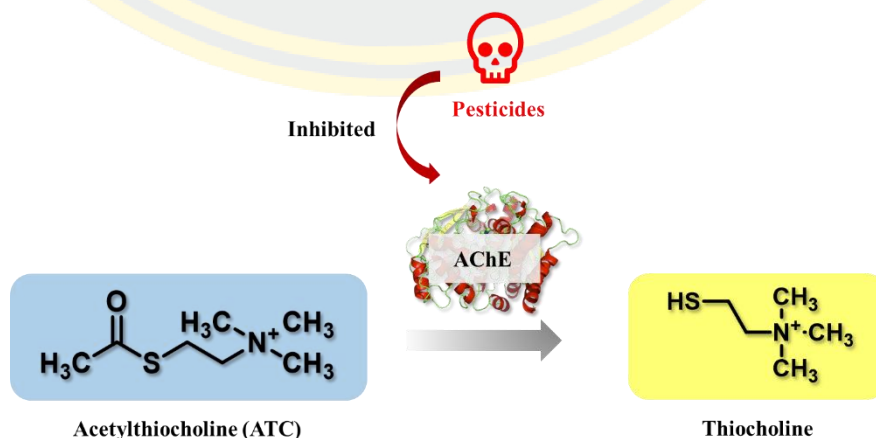
The optimal applied potential for thiol (DTT) detection, range from +0.1 to +0.4 V, was evaluated using hydrodynamic voltammetry by injecting a volume of 3  $\mu$ L of a 1 mM DTT solution into the flow system. All other experimental conditions were kept consistent with the parameters outlined in section 3.7. The signal-to-

baseline ratio (S/B) was plotted as a function of the applied potential to ascertain the appropriate potential, which was subsequently utilized for further experiments.

### 3.8.3.2 Analysis of organophosphate pesticide using the CF- $\mu$ CAD system

To further demonstrate the applicability of the developed system, organophosphate (OP) pesticide was analyzed. The analysis was based on enzyme inhibition assay where the acetylthiocholine was hydrolyzed by acetylcholinesterase (AChE) giving thiocholine (thiol compound similar to DTT) as a product and detected electrochemically using the developed system. Upon the addition of OPs, the AChE activity was inhibited yielding less thiocholine. The reduction of amperometric current was used to quantify OPs in the samples. Pesticide analysis was carried out by adding 20  $\mu$ L of 2 U/mL acetylcholinesterase (AChE) solution to a microtube. Next, a 20  $\mu$ L of CPO at 10 to 100 ng/mL concentrations was added, followed by the 20  $\mu$ L of acetylthiocholine solution with a concentration of 5 mM. The solution was mixed well using a stirrer. Finally, the solution was measured using the developed microflow injection system.

To verify the assay, OP pesticide analysis in water from rice fields was carried out. The samples were collected from the rice fields in various location of Thailand was firstly filtered with a 0.45-micron membrane syringe filter. Each sample was then spiked with three different concentrations of chlorpysifos-oxon (CPO), OP pesticide standard. The samples were subjected to the enzyme inhibition assay with the process described above to determine pesticide in the samples.



Figures 3-5 Detection of organophosphate pesticides is conducted using the CF- $\mu$ CAD system through an enzymatic method.

### ***3.8.3 Analytical features for the analysis of H<sub>2</sub>O<sub>2</sub>, glucose and organophosphate pesticide using the CF- $\mu$ CAD system***

#### ***3.8.3.1 Repeatability***

The experiment was performed by analysis of three replicates of the standard with the concentration in the linear range. The peak heights obtained from the experiment were employed to calculate the percentage relative standard deviation (Relative standard deviation, %RSD), to assess the repeatability of the analysis.

#### ***3.8.3.2 Limit of Detection and Quantification: LOD, LOQ***

The limit of detection (LOD) and limit of quantification (LOQ) are defined as the concentrations of the standard at which the signal is 3 and 10 times the baseline noise, respectively. These parameters are evaluated by analysis of the signal obtained from measurements of baseline noise.

## CHAPTER 4

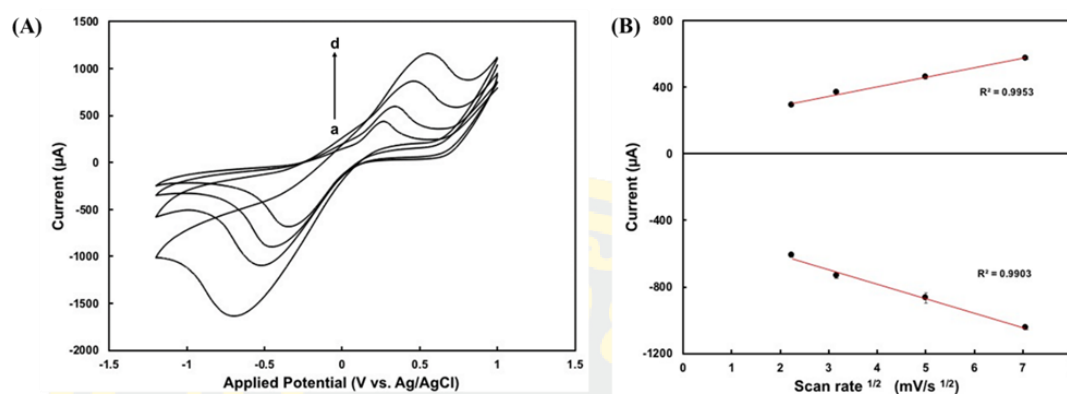
### RESULTS AND DISCUSSION

#### 4.1 Electrochemical characterization on cloth-based sensor by cyclic voltammetry

The electrochemical behavior fabricated on cloth-based devices that used further as a detection platform on the microflow system was first characterized. The electrodes were fabricated on the cloth-based sensor cut to obtain only the electrode region. This test zone allowed for static solution for cyclic voltametric characterization. The working electrode obtained from the carbon paste modified by Prussian Blue (PB-electrode) was evaluated by cyclic voltammetry of the 1 mM KNO<sub>3</sub> supporting electrolyte. As shown in Figures 4-1A, the cyclic voltammogram of the PB (iron(III) hexacyanoferrate(II)) electrode gave both cathodic and anodic peak as a result of the redox reaction of PB as follows(O'Halloran, Pravda, & Guilbault, 2001):



When the scan rate increased from 5 to 50 mV/s, the increasing of the cathodic and anodic peaks were observed and directly proportional to the square root of the scan rate studied (Figures 4-1B). This linearity indicated the mass transfer in this system is a diffusion-controlled process similar to the behavior of traditional electrochemical cells.

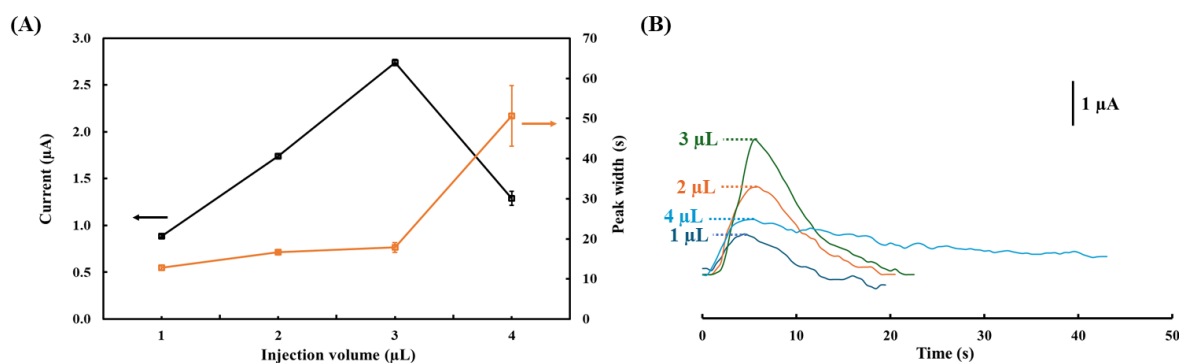


Figures 4-1 (A) Representative cyclic voltammograms of the PB-modified carbon paste electrodes at different scan rates ((a) 5, (b) 10, (c) 25, and (d) 50 mV/s) in 1 M KNO<sub>3</sub>. (B) The relationship between anodic and cathodic currents and the square root of the scan rate.

## 4.2 Microflow injection analysis system optimization

### 4.2.1 Optimum injection volume of sample solution

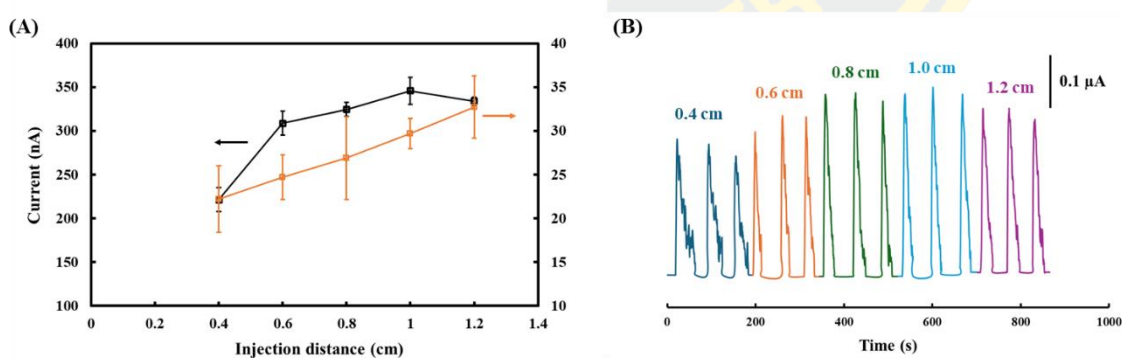
The parameters that impacted on the sensitivity, analysis time and the flow profile of the developed CF- $\mu$ CAD system including sample volume, injection distance and inclined angle were evaluated. The optimization of these parameters was performed using amperometric detection of 1 mM H<sub>2</sub>O<sub>2</sub> as a model standard. The sample injection volume was first investigated as it affected the flow profile and analysis time. (Pradela-Filho et al., 2020) The results showed that as the injection volume increased, the peak height of the reduction current and the peak width also increased. (Moreira, Takeuchi, Richter, & Santos, 2014) However, at the injection volume of 4.0  $\mu$ L, the reduction current decreased with the high peak width (high analysis time per injection) as a result of the band broadening of the high volume sample flow (Figure 4-2). The sample volume of 3.0  $\mu$ L was selected as the optimal injection volume and used for further experiments since it gave high peak current and short analysis time.



Figures 4-2 The relationship between the reduction current (black) and peak width (orange) and the injection volume. (Applied potential:  $-0.30$  V vs Ag/AgCl;  $\text{H}_2\text{O}_2$ : 1.0 mM; Injection distance: 1 cm; Incline angle: 35 degree), (B) The signal of injection volume with amperometry.

#### 4.2.2 Optimum injection distance of sample solution

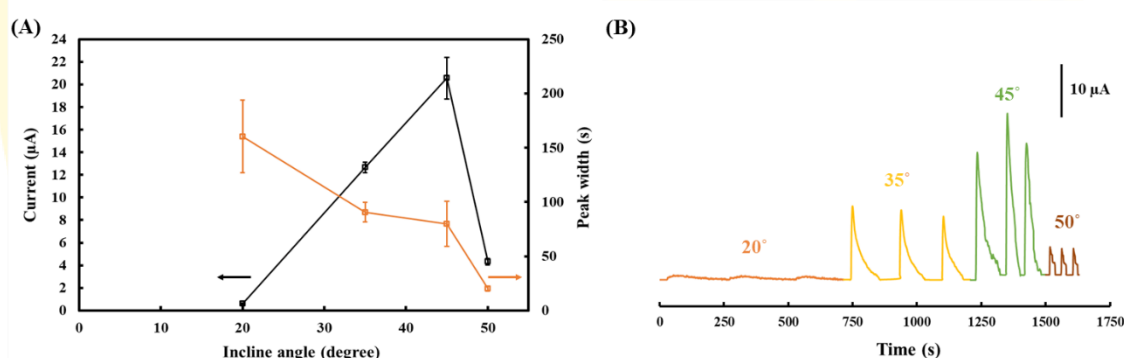
The sample injection distance measured from the working electrode could impact the electrochemical signal (Figures 4-3) and hence were investigated in the range of 0.40- 1.2 cm. From the analysis of 1.0 mM  $\text{H}_2\text{O}_2$ , the injection distance at 1.0 cm provided the highest reduction current where the peak width was similar to other evaluated distance. Shorter injection distance was found to give high noise. Therefore, the injection distance of 1.0 cm was considered as an optimal value and used for further experiments.



Figures 4-3 (A) The relationship between of reduction current (black) and peak width (orange) as a function of sample injection distance (measured from reference electrode). (Applied potential:  $-0.30$  V vs Ag/AgCl;  $\text{H}_2\text{O}_2$ : 1.0 mM; Injection volume: 2.0 μL; Incline angle: 35 degree), (B) The signal of injection distance with amperometry.

### 4.2.3 Optimum Incline angle electrode area of the cloth-based device

Finally, the inclined angle of the developed system was carried out. A solution of 1.0 mM  $\text{H}_2\text{O}_2$  was injected into the sample injection area of the  $\mu\text{CAD}$  which was tilted at the angles of 20, 35, 45 and 50 degrees. As shown in Figures 4-4, the inclined angle of  $\mu\text{CAD}$  increased from 20-45 degree, the higher peak current and the narrower peak was obtained as a result of lower band broadening at the higher flow rate. However, at 50 degree, much lower reduction current with narrower peak width than other conditions was observed as a result of too high flow rate of the sample flow through the electrode causing low amount analyte to undergo redox reaction at electrode surface. At 45 degree, the narrowest peak width and highest reduction current was obtained and hence it was selected as the optimal angle for tilting the  $\mu\text{CAD}$  and used for further experiments.



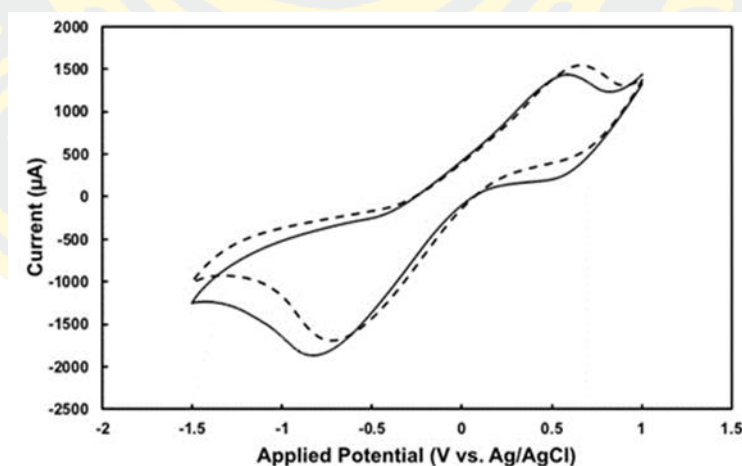
Figures 4-4 (A) Relationship between the reduction current (black) and peak width (orange) and the inclined angle of the  $\mu\text{CAD}$ . (Applied potential:  $-0.30\text{ V}$  vs  $\text{Ag}/\text{AgCl}$ ;  $\text{H}_2\text{O}_2$ : 1.0 mM; Injection distance: 1.0 cm; Injection volume: 3.0  $\mu\text{L}$ ), (B) The signal of inclined angle of the  $\mu\text{CAD}$  with amperometry.

## 4.3 Application of the developed microflow system

The developed CF- $\mu\text{CAD}$  system was used as a continuous analytical platform for detection of  $\text{H}_2\text{O}_2$ , glucose and pesticide to demonstrate the applicability of the developed system for food analysis, clinical application and agricultural detection, respectively. All analyte detection was performed under the same microflow conditions that have been optimized as described above.

#### 4.3.1 Hydrogen peroxide detection using the developed CF- $\mu$ CAD system

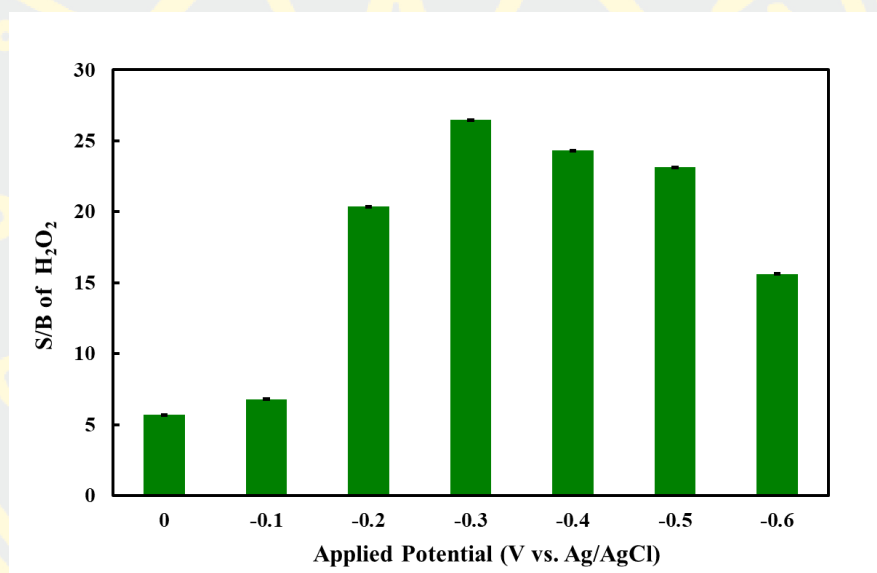
The quantitative analysis of  $\text{H}_2\text{O}_2$  is of significance because it is the product of many highly selective oxidase enzymes.  $\text{H}_2\text{O}_2$  plays an important role in the fields of food industry for its excellent antimicrobial and bactericidal properties, and the residues of  $\text{H}_2\text{O}_2$  in food may result in many adverse effects on humans. (Liu et al., 2022) For detection of  $\text{H}_2\text{O}_2$ , the cyclic voltammetry was first performed to study the electrochemical response of this analyte. The study was carried out with the static condition where the  $\mu$ CAD in the zone containing electrochemical detection zone was cut to generate the test zone that did not allow the solution flow. As shown in Figures 4-5, well-defined responses of the electrochemical signal of both  $\text{KNO}_3$  supporting electrolytes and  $\text{H}_2\text{O}_2$  was observed. The cyclic voltammogram for  $\text{KNO}_3$  solution (dash line) gave both oxidation current and reduction current as a result of the reaction of Prussian blue redox reaction in the working electrode. (Wijitar Dungchai, 2009) In the presence of  $\text{H}_2\text{O}_2$  (solid line), higher reduction current was obtained indicating that the electrochemical detection can be performed using the PB materials and can be further used for the flow system.



Figures 4-5 Cyclic voltammogram obtained from analysis of  $\text{H}_2\text{O}_2$  (solid line) and  $\text{KNO}_3$  (dash line) using the electrodes fabricated on cloth-based devices. Experimental conditions: Scanning potential: -1.2-1 V; Scan rate at 0.05 V/s; Step potential 0.002 V; Supporting electrolyte is  $\text{KNO}_3$  concentration 1 M.

#### 4.3.1.1 Applied potential

Hydrodynamic voltammetry was carried out to find the suitable detection potential of  $\text{H}_2\text{O}_2$  in the flow system. The signal to baseline ratio (S/B) of the flow profile obtained from analysis of 1 mM  $\text{H}_2\text{O}_2$  at each evaluated potential is shown in Figure 4-6. It was found that the highest S/B was obtained at the reduction current of -0.30 V. Higher applied potential gave higher current but also high baseline noise and can cause the interference from other redox active species in the samples. For further studies, a potential of detection of -0.30 V was chosen as it was adequate to detect hydrogen peroxide using the PB electrode in the developed microflow system. (Oliveira et al., 2019)

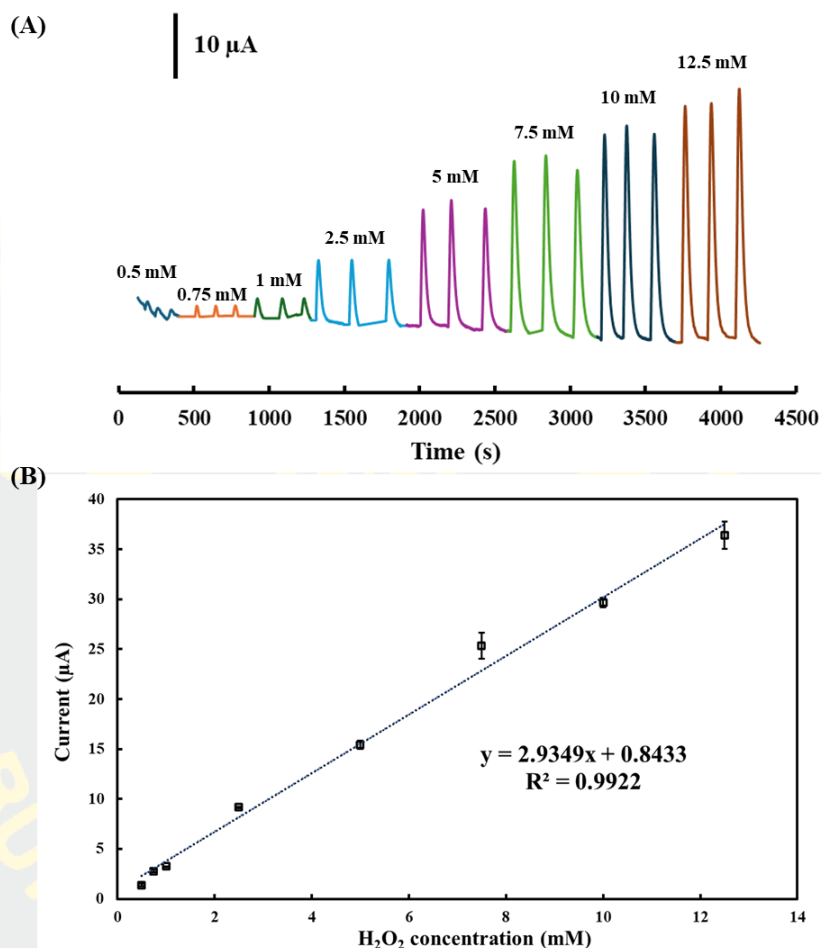


Figures 4-6 Relationship between the signal to blank of  $\text{H}_2\text{O}_2$  and applied potential (V) (Supporting electrolyte: 1 M  $\text{KNO}_3$ , Detection: 1 mM  $\text{H}_2\text{O}_2$ , injection volume: 3  $\mu\text{L}$ , injection distance: 1 cm from RE).

#### 4.3.1.2 Linear range

The analysis of  $\text{H}_2\text{O}_2$  was carried out using the developed CF- $\mu\text{CADs}$ . As shown in Figure 4-7, flow profiles for different concentrations of  $\text{H}_2\text{O}_2$  were obtained where the peak height of the flow profile increased as  $\text{H}_2\text{O}_2$  concentration increased. The plot of reduction current as a function of  $\text{H}_2\text{O}_2$  concentration gave a linear range

of 0.5-12.5 mM. This detection range is similar to other electrochemical method for H<sub>2</sub>O<sub>2</sub> detection. (John Smith, 2020)



Figures 4-7 (A) The signal of H<sub>2</sub>O<sub>2</sub> measured with amperometry. (B) Calibration curve of H<sub>2</sub>O<sub>2</sub> on a cloth-based device with microflow injection analysis. (Experimental conditions: Applied potential: -0.3 V vs. Ag/AgCl; Carrier solution: 1 M KNO<sub>3</sub>; Injection volume: 3 μL; Injection distance: 1.0 cm; Inclined angle: 45 degree, n=3).

#### 4.3.1.3 Repeatability, Limit of Detection, and Limit of Quantification

The limit of detection (LOD) and limit of quantification (LOQ) defined as the concentration that gave signal 3 and 10 times the noise ( $S/N = 3, 10$ ) were found to be 0.46 mM and 0.86 mM respectively. The repeatability evaluated by replicate analysis of H<sub>2</sub>O<sub>2</sub> at the concentration in the linear range was found to have a relative standard

deviation (RSD) in the range of 0.77-9.10% (n=3). The %RSD value obtained is within the accepted standard value. ("Appendix F: Guidelines for Standard Method Performance Requirements," 2016) These results indicated that the developed microflow system has been proven for used as an analytical platform for H<sub>2</sub>O<sub>2</sub> analysis.

To verify the applicability in real-world samples, the analysis of H<sub>2</sub>O<sub>2</sub> in chicken feet samples was carried out. The H<sub>2</sub>O<sub>2</sub> level in unspiked samples was not detected, suggesting that the H<sub>2</sub>O<sub>2</sub> level was less than the LOD (0.46 mM) of the method (Table 4-1). For spiked samples with two concentration levels in the linear range, the recoveries were close to 100%, indicating that the developed platform is feasible and accurate for H<sub>2</sub>O<sub>2</sub> detection in real-world samples. ("Appendix F: Guidelines for Standard Method Performance Requirements," 2016)

Table 4-1 Analysis of H<sub>2</sub>O<sub>2</sub> in chicken feet samples by the CF- $\mu$ CAD platform.

Sample	Spiked H <sub>2</sub> O <sub>2</sub> (mM)	Found (mM) $\pm$ SD (n=3)	Recovery (%)
Chicken feet	0	N.D.	-
	3	2.83 $\pm$ 0.05	94
	5	4.88 $\pm$ 0.07	98

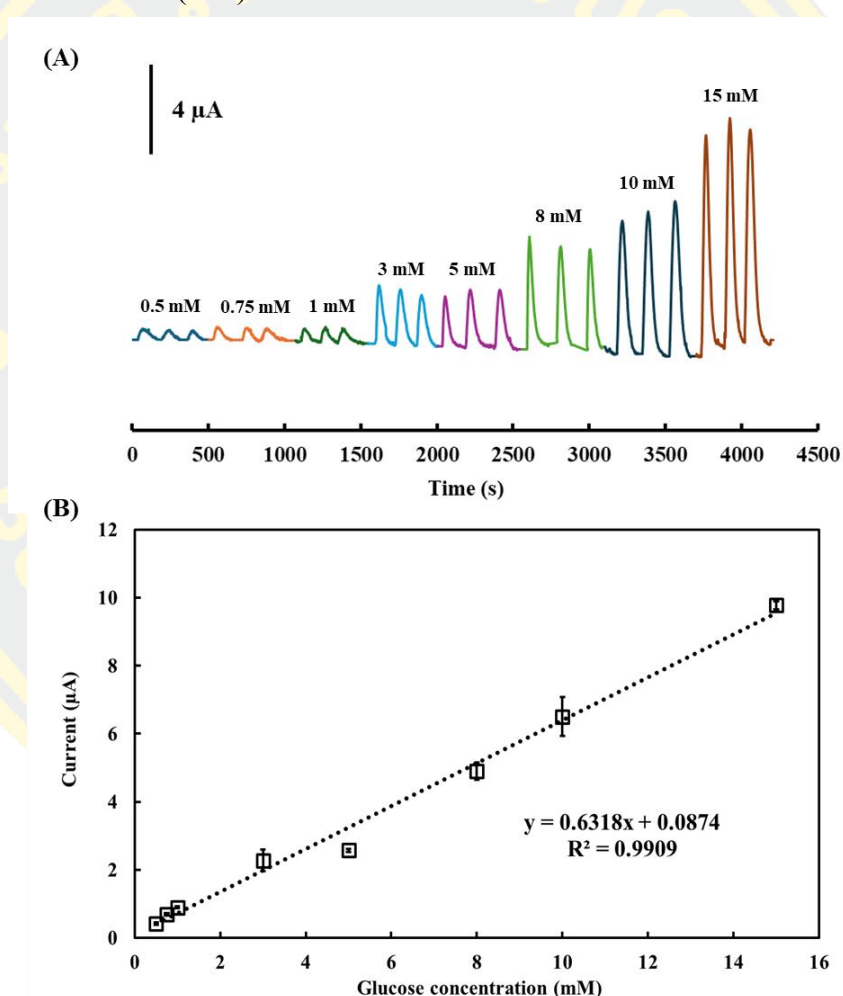
N.D.: Not detected

#### 4.3.2 Glucose detection using the developed CF- $\mu$ CAD system

The platform was further employed for glucose analysis in human control serum to demonstrate its application in medical diagnostics. The excessive glucose level in human blood is considered as an important feature of diabetic patients which can lead to a series of complications that seriously threaten human health, including heart disease, kidney failure, and blindness. (Qi et al., 2013) The glucose was analyzed based on the enzymatic oxidation of glucose by glucose oxidase yielding H<sub>2</sub>O<sub>2</sub> and gluconic acid. The produced H<sub>2</sub>O<sub>2</sub> was detected electrochemically using the conditions for H<sub>2</sub>O<sub>2</sub> detection as described above.

### 4.3.2.1 Linear range

The analysis of glucose at different concentrations gave different peak current where the higher the concentration, the higher the reduction current. A plot of peak current as a function of glucose concentration gave a linear calibration curve from 0.5 to 15 mM. This range is suitable for the analysis of glucose in serum with both normal level (3.5–5.3 mM) and abnormal level (>7 mM). The repeatability obtained from the replicate analysis of glucose with the concentration in the linear range was in the range of 1.21–13.83% (n=3).



Figures 4-8 (A) The signal of glucose solution measured with amperometry. (B) Calibration curve of glucose on a cloth-based device with microflow injection analysis. (Experimental conditions: Applied potential: -0.3 V vs. Ag/AgCl; Carrier solution: 1 M KNO<sub>3</sub>; Injection volume: 3 μL; Injection distance: 1.0 cm; Inclined angle: 45 degree, n=3)

#### ***4.3.2.2 Limit of Detection and Limit of Quantification***

The limit of detection (LOD) achieved using the developed CF- $\mu$ CAD system for glucose analysis was determined to be 0.42 mM. which is comparable in performance to conventional blood glucometers that can detect levels as low as 1.7 mM.(Magner, 1998)

#### ***4.3.2.3 Glucose in human control serum analysis using the developed CF- $\mu$ CAD system***

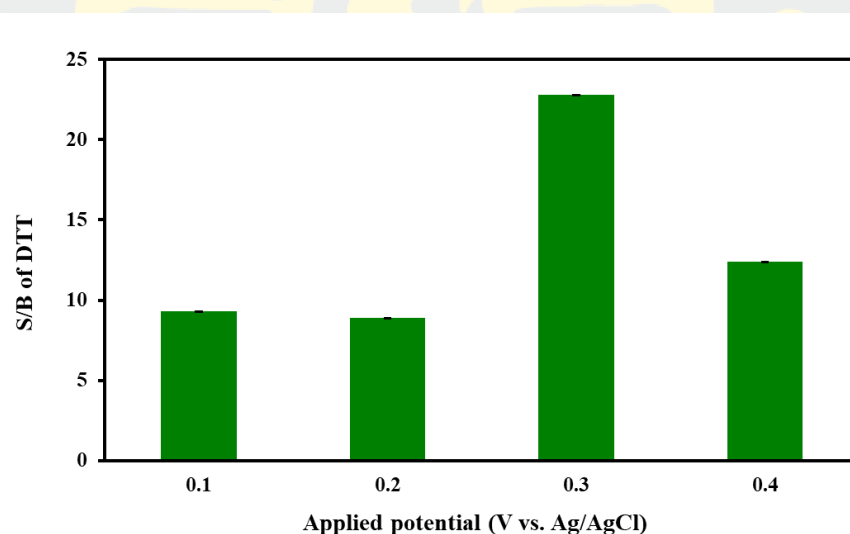
The analysis of glucose in human control serum including HumaTrol N (normal range) and HumaTrol P (abnormal range) (Human GmbH, Germany) using the developed CF- $\mu$ CAD system was carried out. The measured glucose level in normal range was  $6.61 \pm 0.61$  mM (n=3) (Certified value: 5.65 mM) and abnormal range was  $12.42 \pm 0.49$  mM (n=3) (Certified value: 12.3 mM). From the statistical t-test, the concentrations of glucose obtained from the CF- $\mu$ CAD system were not significant difference at the 95% confidence level from the certified values obtained in clinical control samples, both in normal (One-sample t-test, two tailed  $P = 0.11$ ) and abnormal ranges (One-sample t-test, two tailed  $P = 0.71$ ). These values indicates that the CF- $\mu$ CAD system developed is appropriate for analysis of glucose in serum samples.

#### ***4.3.3 Pesticide analysis using the developed CF- $\mu$ CAD system***

Finally, the analysis of organophosphate pesticide (OP) in rice field water samples was carried out using the developed platform to demonstrate the applicability in agricultural area.(Ghassempour, Mohammadkhah, Najafi, & Rajabzadeh, 2002) The analysis was based on the enzyme inhibition assay. In the absence of OP pesticide, the AChE catalytically hydrolyzed ATC giving thiocholine, a thiol molecule as a product. In the presence of OP pesticide, the activity of AChE was inhibited giving less activity to catalyze ATC and hence, giving less thiocholine. By monitoring the amount of thiocholine, the OP pesticide can be quantified.

#### 4.3.3.1 Applied potential

In this work, the detection of thiol representative molecule such as DTT was first investigated to ensure that the system can be used to quantify the thiocholine product from the enzyme inhibition assay. The hydrodynamic voltammetry of DTT was carried out in the applied potential range of +0.10 V and +0.40 V to find suitable applied potential for thiol detection in the developed microflow system. The results showed that the highest S/B ratio at applied potential of +0.3 V was observed and selected as optimal value for thiol detection since it was sufficient to generate the reaction and increase the electrocatalysis of the thiol by PB electrode. This detection potential was similar to the applied potential for DTT analysis in the microflow system made by polydimethylsiloxane (PDMS) using the carbon paste electrode modified by cobalt phthalocyanine as electrocatalyst. (Kalinke et al., 2019; Sameenoi et al., 2012)

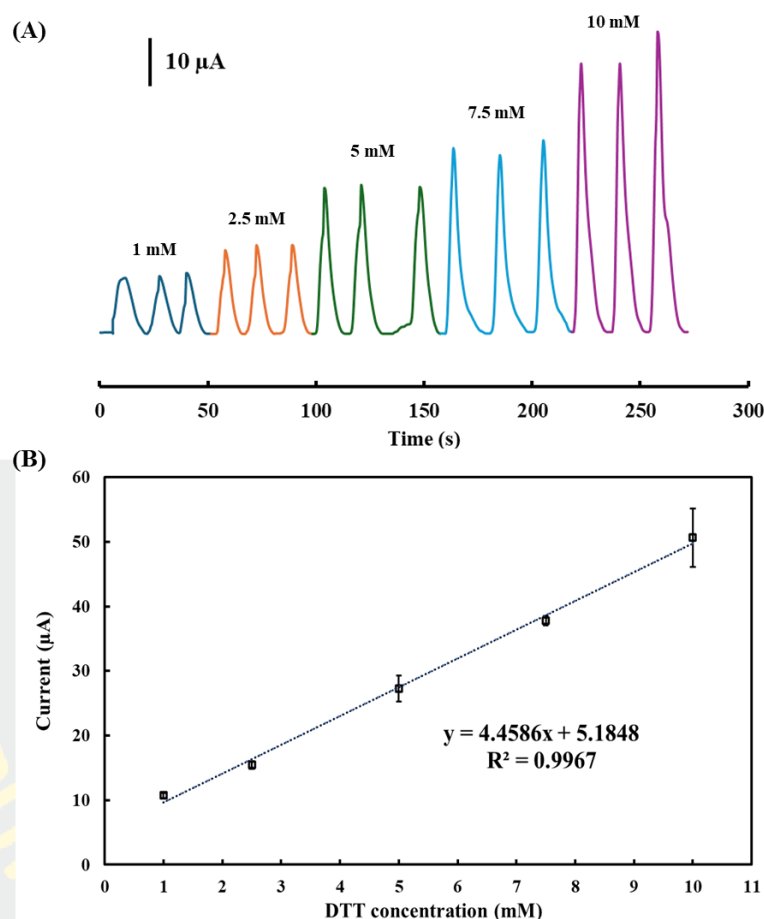


Figures 4-9 Relationship between the signal to blank of DTT and applied potential (V) (Supporting electrolyte: 1 M  $\text{KNO}_3$ , Detection: 1 mM  $\text{H}_2\text{O}_2$ , injection volume: 3  $\mu\text{L}$ , injection distance: 1 cm from RE).

#### 4.3.3.2 Linear range

Next, DTT analysis at different concentration was carried out under optimal conditions. Flow profiles were obtained for different concentrations of DTT where the

peak height of the flow profile increased with increasing DTT concentration. The graph of the oxidation current as a function of DTT concentration gave a linear range of 1.0-10.0 mM.



Figures 4-10 (A) The signal of dithiothreitol solution measured with amperometry. (B) Calibration curve of dithiothreitol on a cloth-based device with microflow injection analysis. (Experimental conditions: Applied potential: +0.3 V vs. Ag/AgCl; Carrier solution: 1 M KNO<sub>3</sub>; Injection volume: 3 μL; Injection distance: 1.0 cm; Inclined angle: 45 degree, n=3).

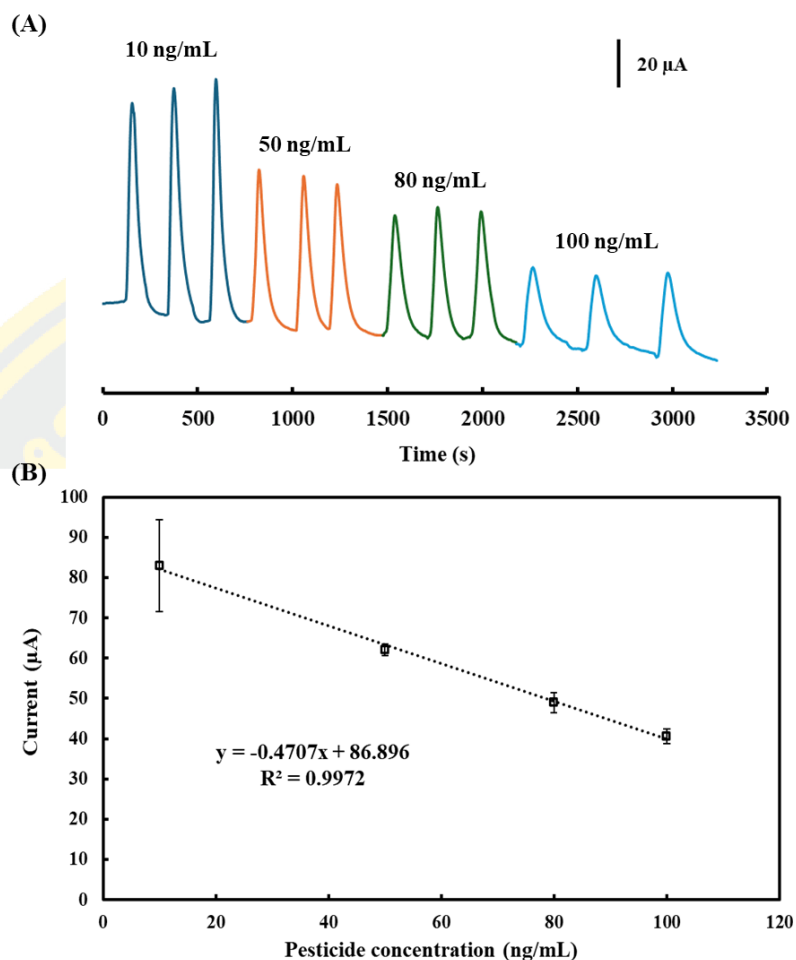
#### 4.3.3.3 Limit of Detection and Limit of Quantification

The limit of detection (LOD) and limit of quantification (LOQ) defined as the concentration that gave signal 3 and 10 times the noise ( $S/N = 3, 10$ ) were found to be 1.30 mM and 1.63 mM respectively. The repeatability evaluated by replicate analysis

of thiol at the concentration in the linear range was found to have a relative standard deviation (RSD) in the range of 1.98-8.87% (n=3). The %RSD value obtained is within the accepted standard value. These results indicated that the detection of thiocholine products is possible using the conditions similar to the DTT detection.

#### ***4.3.3.4 Analysis of organophosphate pesticide using the CF- $\mu$ CAD system***

Next, the analysis of pesticide was investigated using the enzyme inhibition assay. After mixed with the AChE and ATC, the chlorpysifos-oxon (CPO) used as model standard OP pesticide was analyzed by monitoring the decreasing of thiocholine using the developed CF- $\mu$ CAD platform. As the pesticide concentration increased, the flow profile of the thiocholine signal decreased giving the pesticide calibration curve in a dose-response manner. The linear calibration was obtained in the range of 10-100 ng/mL indicating that the analysis of pesticide using the developed platform can be applied for quantitation of low-level pesticide.



Figures 4-11 (A) The signal of chlorpyrifos-oxon (CPO) solution measured with amperometry. (B) Calibration curve of pesticide on a cloth-based device with microflow injection analysis. (Experimental conditions: Applied potential: -0.3 V vs. Ag/AgCl; Carrier solution: 1 M KNO<sub>3</sub>; Injection volume: 3 μL; Injection distance: 1.0 cm; Inclined angle: 45 degree, n=3).

To demonstrate the application in real-world samples, water samples collected from the rice field in Chonburi, Thailand were analyzed for pesticides. The extensive use of pesticides is associated with modern agricultural practices aimed at ensuring food security, and the application of pesticides to rice constitutes the third-largest use globally. (Anyusheva, Lamers, La, Nguyen, & Streck, 2016; Sruthi, Shyleshchandran, Mathew, & Ramasamy, 2017) As shown in Table 4-2, the unspiked samples

contained some of the pesticide indicating the extensive use of pesticides to increase yield in rice cultivation. From the spiked samples, the recovery was found in the acceptable value set by AOAC indicating no significant interference from species present in the matrix of the water samples from the rice field.

Table 4-2 Analysis of Thiol in samples by the developed method.

<b>Sample</b>	<b>Spiked pesticide (ng/mL)</b>	<b>Found (ng/mL) ± SD (n=3)</b>	<b>Recovery (%)</b>
<b>Water samples from rice fields</b>	0	73.05 ± 3.71	-
	20	91.68 ± 1.65	93
	50	115.19 ± 1.65	84

## CHAPTER 5

### CONCLUSIONS AND FUTURE PERSPECTIVES

#### 5.1 Conclusions

The CF- $\mu$ CADs were successfully developed and demonstrated for use as continuous microflow injection analysis with low sample and reagent consumptions. The electrodes were fabricated using a screen-printing technique with a PVC template on a cloth-based device. The electrodes incorporated on the cloth-based device consist of a reference electrode, a working electrode, and an auxiliary electrode made by silver-silver chloride, carbon paste mixed with Prussian blue and pure carbon paste, respectively. Optimal parameters affecting the flow analysis were investigated including injection volume, injection distance, and inclined angle. Under optimal conditions, the analysis of  $H_2O_2$ , glucose and pesticide were carried out giving excellent flow profiles. Subsequently, this method was applied to real samples, including chicken feet and water from rice fields, yielding favorable results. Therefore, the developed microflow injection system could be further used as analytical platform for a wide range of application.

#### 5.2 Future perspective

The future study will be focused on the electrode material modification for selective application for interested analytes. Surface of the cotton cloth will also be modified in order to study the possibility to use as a chromatographic platform for chemical separation.

## REFERENCES

- Agustini, D., Bergamini, M. F., & Marcolino-Junior, L. H. (2016). Characterization and optimization of low cost microfluidic thread based electroanalytical device for micro flow injection analysis. *Anal Chim Acta*, *951*, 108-115.  
doi:10.1016/j.aca.2016.11.046
- Ahmed, S., et al. (2021). Paper-based microfluidic devices: Emerging themes and applications. *Analytical Chemistry*, *93*(2), 314-338.  
doi:10.1021/acs.analchem.0c04523
- Anyusheva, M., Lamers, M., La, N., Nguyen, V. V., & Streck, T. (2016). Persistence and leaching of two pesticides in a paddy soil in northern Vietnam. *Clean-soil, air, water*, *44*(7), 858-866.
- Appendix F: Guidelines for Standard Method Performance Requirements. (2016). *AOAC Official Methods of Analysis*.
- Cerdà, V., Ferrer, L., Avivar, J., & Cerdà, A. (2014). Evolution and Description of the Principal Flow Techniques. In *Flow Analysis* (pp. 1-42).
- Chen, Y., et al. (2021). Cloth-based analytical devices: Fabrication methods, applications, and future perspectives. *Analytica Chimica Acta*, *1165*, 338474.  
doi:10.1016/j.aca.2020.338474
- Ghassempour, A., Mohammadkhah, A., Najafi, F., & Rajabzadeh, M. (2002). Monitoring of the pesticide diazinon in soil, stem and surface water of rice fields. *Analytical sciences*, *18*(7), 779-783.
- Godino, N., Gorkin, R., 3rd, Bourke, K., & Ducree, J. (2012). Fabricating electrodes for amperometric detection in hybrid paper/polymer lab-on-a-chip devices. *Lab Chip*, *12*(18), 3281-3284. doi:10.1039/c2lc40223h
- Gonzalez, C., et al. (2018). Rapid determination of amino acids in food products using microflow injection analysis with fluorescence detection. *Food Chemistry*, *245*, 1164-1171. doi:DOI: 10.1016/j.foodchem.2017.11.109
- Guan, W., Zhang, C., Liu, F., & Liu, M. (2015). Chemiluminescence detection for microfluidic cloth-based analytical devices (muCADs). *Biosens Bioelectron*, *72*, 114-120. doi:10.1016/j.bios.2015.04.064
- Jane Doe, J. S. (2020). Development of portable microfluidic devices: Recent advances and applications. *Analytica Chimica Acta*, *1138*, 1-18.  
doi:10.1016/j.aca.2020.09.021
- John Smith, M. J., David Lee. (2020). Development of a Screen-Printed Electrode Modified with Manganese Dioxide Nanoparticles for Hydrogen Peroxide Determination. *Electroanalysis*, *30*(2), 123-135.
- Jonathan S. Daniels, J. K. B. C. (2019). Microfluidic technology: developments and applications in neurobiology. *Current Opinion in Neurobiology*, *55*, 86-93.  
doi:10.1016/j.conb.2018.12.008
- Kalinke, C., Wosgrau, V., Oliveira, P. R., Oliveira, G. A., Martins, G., Mangrich, A. S., . . . Marcolino-Junior, L. H. (2019). Green method for glucose determination using microfluidic device with a non-enzymatic sensor based on nickel oxyhydroxide supported at activated biochar. *Talanta*, *200*, 518-525.  
doi:10.1016/j.talanta.2019.03.079
- Li, Y., et al. (2018). Versatile microflow injection analysis coupled with capillary electrophoresis for amino acid analysis. *Electrophoresis*, *39*(13), 1667-1673.

- doi:10.1002/elps.201700469
- Liu, S. G., Liu, S., Yang, S., Zhao, Q., Deng, J., & Shi, X. (2022). A facile fluorescent sensing strategy for determination of hydrogen peroxide in foods using a nanohybrid of nanoceria and carbon dots based on the target-promoted electron transfer. *Sensors and Actuators B: Chemical*, 356, 131325.
- Magner, E. (1998). Trends in electrochemical biosensors. *Analyst*, 123(10), 1967-1970. doi:10.1039/a803314e
- Maria A. G. Soliva, M. B. M., Vladislav A. Pavlov. (2017). Microflow Injection Analysis: A Review. *ANALYTICAL SCIENCES*, 33(9), 1077-1090. doi:10.2116/analsci.33.1077
- Moreira, B. C. S., Takeuchi, R. M., Richter, E. M., & Santos, A. L. (2014). Development of a Flow Injection Analysis System Employing Alternative and Low-Cost Materials for Didactic Purposes. *Química Nova*. doi:10.5935/0100-4042.20140194
- Muhammad Rizwan Javed, M. Z.-U.-H., Faqir Muhammad Anjum, Saima Naz, Ramsha Sattar, Humaira Nadeem, Tanveer Akhtar. (2018). Microfluidic flow injection analysis: Recent applications in pharmaceutical, environmental, and biological analysis. *Journal of Pharmaceutical and Biomedical Analysis*, 152, 186-197. doi:10.1016/j.jpba.2017.11.023
- Nilghaz, A., Wicaksono, D. H., Gustiono, D., Abdul Majid, F. A., Supriyanto, E., & Abdul Kadir, M. R. (2012). Flexible microfluidic cloth-based analytical devices using a low-cost wax patterning technique. *Lab Chip*, 12(1), 209-218. doi:10.1039/c1lc20764d
- O'Halloran, M. P., Pravda, M., & Guilbault, G. G. (2001). Prussian Blue bulk modified screen-printed electrodes for H<sub>2</sub>O<sub>2</sub> detection and for biosensors. *Talanta*, 55(3), 605-611. doi:[https://doi.org/10.1016/S0039-9140\(01\)00469-6](https://doi.org/10.1016/S0039-9140(01)00469-6)
- Oliveira, M. C., Watanabe, E. Y., Agustini, D., Banks, C. E., Marcolino-Júnior, L. H., & Bergamini, M. F. (2019). Nonenzymatic sensor for determination of glucose in blood plasma based on nickel oxyhydroxide in a microfluidic system of cotton thread. *Journal of Electroanalytical Chemistry*, 840, 153-159. doi:10.1016/j.jelechem.2019.03.038
- Peter R. Seidl, A. M. (1994). Microflow Injection Analysis: Principles, Instrumentation, and Applications. *Analytical Chemistry*, 66(23), 455A-462A. doi:10.1021/ac00095a732
- Pradela-Filho, L. A., Noviana, E., Araujo, D. A. G., Takeuchi, R. M., Santos, A. L., & Henry, C. S. (2020). Rapid Analysis in Continuous-Flow Electrochemical Paper-Based Analytical Devices. *ACS Sens*, 5(1), 274-281. doi:10.1021/acssensors.9b02298
- Qi, B., Yang, H., Zhao, K., Bah, M. M., Bo, X., & Guo, L. (2013). Three-dimensional macroporous Cu electrode: Preparation and electrocatalytic activity for nonenzymatic glucose detection. *Journal of Electroanalytical Chemistry*, 700, 24-29. doi:<https://doi.org/10.1016/j.jelechem.2013.04.002>
- Radha S.P. Malon, K.Y. Chua, Wicaksono, D. H. B., & Córcoles, a. E. P. (2012). Cotton Fabric-based Electrochemical Device for Lactate Measurement in Saliva. *The Royal Society of Chemistry*, 0, 1-3. doi:10.1039/x0xx00000x
- Sameenoi, Y., Koehler, K., Shapiro, J., Boonsong, K., Sun, Y., Collett Jr, J., . . . Henry, C. S. (2012). Microfluidic electrochemical sensor for on-line monitoring of

- aerosol oxidative activity. *Journal of the American Chemical Society*, 134(25), 10562-10568.
- Silva, R. M., et al. (2018). Development and validation of a microflow injection analysis method for determination of antibiotics in surface waters. *Journal of Chromatography A*, 1532, 123-131. doi:DOI: 10.1016/j.chroma.2017.12.005
- Sruthi, S., Shyleshchandran, M., Mathew, S. P., & Ramasamy, E. (2017). Contamination from organochlorine pesticides (OCPs) in agricultural soils of Kuttanad agroecosystem in India and related potential health risk. *Environmental Science and Pollution Research*, 24, 969-978.
- Tasaengtong, B., & Sameenoi, Y. (2020a). A one-step polymer screen-printing method for fabrication of microfluidic cloth-based analytical devices. *Microchemical Journal*, 158. doi:10.1016/j.microc.2020.105078
- Tasaengtong, B., & Sameenoi, Y. (2020b). A one-step polymer screen-printing method for fabrication of microfluidic cloth-based analytical devices. *Microchemical Journal*, 158, 105078. doi:<https://doi.org/10.1016/j.microc.2020.105078>
- Wang, J., Huang, T., Shao, M., Yang, S., Luo, L., Zeng, L., & ... & Chen, H. (2021). 3D-printed microfluidic chip for glucose detection with integrated amperometric biosensors. *Sensors and Actuators B: Chemical*, 329, 129-205.
- Wang, Y., Zhu, Y., Huang, Q., Li, L., & Li, Y. (2019). A microfluidic device based on a nanoporous gold electrode for amperometric detection of hydrogen peroxide. *Microchimica Acta*, 186(1), 1-8.
- Wijitar Dungchai, O. C., and Charles S. Henry. (2009). Electrochemical Detection for Paper-Based Microfluidics. *Analytical Chemistry*, 81.
- Zhang, C., Su, Y., Liang, Y., & Lai, W. (2020). Microfluidic cloth-based analytical devices: Emerging technologies and applications. *Biosens Bioelectron*, 168, 112391. doi:10.1016/j.bios.2020.112391



## **BIOGRAPHY**

**NAME** Miss. Tanapron Boonnikom

**DATE OF BIRTH** 26 June 2000

**PLACE OF BIRTH** Ang Tong, Thailand

**PRESENT ADDRESS** 48 Moo.1, Tambon khok chang, Amphoe phakhai,  
Ayutthaya, 13120

**EDUCATION** 2018-2022 Bachelor Science of Chemistry (B.Sc),  
Faculty of Science, Burapha University, Thailand

